



Sluggish Hadean geodynamics: Evidence from coupled $^{146,147}\text{Sm}$ – $^{142,143}\text{Nd}$ systematics in Eoarchean supracrustal rocks of the Inukjuak domain (Québec)



G. Caro^{a,b,*}, P. Morino^a, S.J. Mojzsis^{b,c}, N.L. Cates^b, W. Bleeker^d

^a Centre de Recherches Pétrographiques et Géochimiques (CRPG), UMR 7358, Université de Lorraine, CNRS, 54500 Vandœuvre-lès-Nancy, France

^b Collaborative for Research in Origins (CRiO), Department of Geological Sciences, University of Colorado, UCB 399, 2200 Colorado Avenue, Boulder, CO 80309-0399, USA

^c Institute for Geological and Geochemical Research, Research Center for Astronomy and Earth Sciences, Hungarian Academy of Sciences, 45 Budaörsi Street, H-1112 Budapest, Hungary

^d Geological Survey of Canada, Natural Resources Canada, 601 Booth Street, Ottawa, Ontario K1A 0E8, Canada

ARTICLE INFO

Article history:

Received 7 June 2016

Received in revised form 14 September 2016

Accepted 28 September 2016

Available online 22 October 2016

Editor: M. Bickle

Keywords:

^{146}Sm – ^{142}Nd

Hadean

magma ocean

sluggish tectonics

Ukaliq

Nuvvuagittuq

ABSTRACT

The discovery of deficits in $^{142}\text{Nd}/^{144}\text{Nd}$ in mafic rocks of the Nuvvuagittuq supracrustal belt (NSB) has triggered a debate about the possible preservation of Hadean (pre-3.85 Ga) crustal remnants in the little-known but areally extensive Innuksuac complex (3.6–3.8 Ga, Inukjuak domain, Northeast Superior Province, Canada). Geochronological investigations in the NSB, however, are hampered by the poor preservation and highly disturbed isotopic record of various mafic (amphibolite) lithologies that host the ^{142}Nd anomalies. Here we present ^{146}Sm – ^{142}Nd and ^{147}Sm – ^{143}Nd data for rocks of extrusive magmatic and sedimentary protoliths from the Ukaliq supracrustal belt, a newly discovered volcano-sedimentary enclave enclosed in granitoid gneisses of the Inukjuak domain. Our study also includes the first ^{146}Sm – ^{142}Nd data for quartz-magnetite rocks (banded iron-formation; BIF) of the NSB and the Eoarchean Isua supracrustal belt (ISB) in southern West Greenland. We show that Ukaliq amphibolites carry variably negative ^{142}Nd anomalies, ranging from 0 to –10 ppm, which are positively correlated with their Sm/Nd ratio. If considered as an isochron relationship, the ^{146}Sm – ^{142}Nd array yields an apparent Hadean emplacement age of 4215^{+50}_{-76} Ma. The negative ^{142}Nd anomalies, however, appear to be mainly restricted to amphibolites with boninitic affinities, likely reflecting inheritance from an enriched mantle source. In contrast, tholeiitic and ultramafic lavas have normal $\mu^{142}\text{Nd}$ regardless of their Sm/Nd ratio. Furthermore, BIF from Ukaliq and Nuvvuagittuq lack the negative ^{142}Nd anomalies that should have been produced by in situ decay of ^{146}Sm had these sediments been deposited prior to ca. 4.1 Ga. Instead, they exhibit $\mu^{142}\text{Nd}$ identical to that measured in Isua BIF. Collectively, our results suggest that the ^{146}Sm – ^{142}Nd array characterizing mafic lithologies of Ukaliq and Nuvvuagittuq is an inherited signature with doubtful chronological significance. We interpret the volcanic protoliths of the Innuksuac complex to have been produced by metasomatically triggered melting of a variably enriched Eoarchean mantle, following addition of felsic melts and/or fluids derived from a foundering Hadean mafic crust. Application of coupled $^{146,147}\text{Sm}$ – $^{142,143}\text{Nd}$ chronometry to Ukaliq lavas yields a model age of differentiation of $4.36^{+0.05}_{-0.06}$ Ga for this Hadean precursor. This is similar to late-stage crystallization ages inferred for the lunar and terrestrial magma oceans. The long-term preservation of Earth's primordial crust points to subdued lithospheric recycling in the post-magma ocean Earth.

© 2016 Elsevier B.V. All rights reserved.

1. Introduction

In the absence of an actual rock record of the first 500 Myr of Earth's history – as opposed to detrital Hadean zircons separated from their parent rocks (e.g. Mojzsis et al., 2001) – direct

constraints on the composition, dynamics, and ultimate fate of the primordial lithosphere remain out of reach. Alternatively, indirect studies of the daughter products of short-lived radioactive nuclides show that the silicate Earth experienced early (4.4–4.5 Ga) differentiation (Harper and Jacobsen, 1992; Bennett et al., 2007; Boyet and Carlson, 2005; Boyet et al., 2003; Caro et al., 2003), most likely due to the crystallization of a deep magma ocean in the aftermath

* Corresponding author.

E-mail address: caro@crpg.cnrs-nancy.fr (G. Caro).

of the Moon-forming giant impact. By analogy to the lunar magma ocean model, it has been suggested that Earth's primordial crust was produced via upward migration and crystallization of mafic/ultramafic residual liquids in the final stages of solidification of the uppermost mantle (Caro et al., 2005; Bourdon and Caro, 2007; Rizo et al., 2011). Whereas various chronological aspects of these early events continue to be refined, the fate of Earth's primordial silicate reservoirs and the extent to which magma ocean processes subsequently influenced the geodynamic evolution of our planet, is enigmatic. Geochemical and isotopic studies of Jack Hills zircons suggest that magma ocean crystallization was rapidly followed by the onset of crustal formation processes akin to those operating in the modern Earth (e.g. Harrison, 2009). Precious little is known beyond this, however, about the geodynamic processes by which the primordial lithosphere was returned to the mantle, or the timescale associated with it.

The question of the rise (and demise) of the terrestrial proto-crust is intrinsically connected to that of the geodynamic regime prevailing in the Hadean. A common view, based mostly on petrological and structural arguments, is that subduction (*sensu stricto*) was inoperative until the late Archean (Shirey and Richardson, 2011; Bédard et al., 2003) and that renewal of the Earth's crust before that time operated in a “vertical tectonic” regime (Robin and Bailey, 2009). This view is supported by thermal evolution models which predict that in the hot early Earth mantle melting would have taken place at greater depth than today, generating a thicker crust associated with a highly depleted lithospheric mantle (Johnson et al., 2013; Korenaga, 2006; Vlaar et al., 1994; Sleep and Windley, 1982). Consequently, the Hadean lithosphere was likely stiffer and more buoyant, inhibiting the development of subduction zones and favoring instead a sluggish tectonic style characterized by slower plate motion and an overall longer crustal residence time (Korenaga, 2006; Foley et al., 2014). Alternatively, hotter mantle temperatures may have pushed the young Earth into a stagnant-lid regime (O'Neill and Debaille, 2014), where the mantle is overlain by a mechanically strong and generally immobile lithosphere, and crustal recycling only takes place during episodic pulses of rapid subduction. Lastly, gravitational instabilities in the thickened Hadean crust may have caused catastrophic episodes of rapid foundering and rejuvenation of the entire lithosphere (van Thienen et al., 2004).

The main obstacle to distinguishing these very different scenarios is the paucity of reworked Hadean components in the Archean rock record. In this context, the presence of deficits in $^{142}\text{Nd}/^{144}\text{Nd}$ in magmatic rocks of the Nuvvuagittuq supracrustal belt (NSB), within the Archean Innuksuac gneiss complex (North-eastern Superior province, Quebec), has major implications for our understanding of Hadean geodynamics (O'Neil et al., 2008; Roth et al., 2013). Due to the short half-life of ^{146}Sm ($T_{1/2} = 103$ Myr), ^{142}Nd heterogeneities can only have been produced prior to about 4.1 Ga, and, therefore, are specifically related to mantle–crust differentiation in the Hadean (e.g. Caro, 2011). As Nd is more incompatible than Sm, enriched silicate reservoirs such as Earth's Hadean crust would be characterized by relatively low Sm/Nd ratios, resulting in the development of negative ^{142}Nd anomalies (low $^{142}\text{Nd}/^{144}\text{Nd}$), whereas the complementary depleted mantle would develop positive ^{142}Nd anomalies. The ubiquitous presence of negative ^{142}Nd anomalies in mafic lithologies of the NSB has thus raised the question of whether actual Hadean volcano-sedimentary sequences are preserved in the Inukjuak domain, or if this terrane instead inherited the geochemical fingerprint of a long vanished Hadean reservoir (O'Neil et al., 2008; Roth et al., 2013; Guitreau et al., 2014).

Innate negative ^{142}Nd anomalies from reworked Hadean components have also been reported from granitoids and mafic rocks

of the Acasta gneisses (3.96 Ga, Slave craton, Canada, Mojzsis et al., 2014; Roth et al., 2014), the Schapenburg komatiite (Puchtel et al., 2016) and some 3.4 Ga Ameralik dykes of Southwest Greenland (Rizo et al., 2012). Likewise, the negative ^{142}Nd anomalies carried by Eoarchean tonalite–trondhjemite–granodiorite (TTG) rocks associated with the NSB (i.e. the Voizez suite) provide clear evidence for a variable degree of geochemical inheritance in plutonic rocks of the Innuksuac complex (O'Neil et al., 2008, 2013; Roth et al., 2013). At odds with this interpretation, O'Neil et al. (2008) proposed that the NSB still contains vestiges of the Hadean precursor in which the ^{142}Nd effect was produced, present as a heterogeneous package of highly altered mafic rocks (cummingtonite-rich amphibolite) colloquially termed by them the “Ujaraaluk unit” (O'Neil et al., 2011). This interpretation relies on the argument that NSB cummingtonite-amphibolites exhibit $^{142}\text{Nd}/^{144}\text{Nd}$ signatures that positively correlate with their Sm/Nd ratio (O'Neil et al., 2008). This characteristic was observed neither in the Acasta, Schapenburg, or Ameralik rocks cited above, and as such could be taken to represent a disturbed yet geochronologically significant isochron relationship. If the interpretation of O'Neil and co-workers is correct, then the volcano-sedimentary sequence of the NSB would represent the oldest preserved crust on Earth, and accordingly its geochemical record would have the potential to constrain the geodynamic and environmental state of our planet to within less than 300 Myr after the Moon-forming event.

Yet, the interpretation of the ^{146}Sm – ^{142}Nd signal as a true isochron in the NSB rocks is not without caveats. First, the chronological constraints provided by the ^{147}Sm – ^{143}Nd and ^{146}Sm – ^{142}Nd chronometers are in fact strongly discordant; the cummingtonite-amphibolites define a younger ^{147}Sm – ^{143}Nd errorchron at ca. 3.6 Ga (O'Neil et al., 2012), and the apparent decoupling of the two Sm–Nd chronometers is not well understood (O'Neil et al., 2012; Roth et al., 2013). Second, quartz–biotite schists and quartzites of probable detrital origin from the NSB show robust detrital zircon populations in a 3.65–3.78 Ga range, inconsistent with deposition in the Hadean (David et al., 2006; Cates and Mojzsis, 2007; Cates et al., 2013; Darling et al., 2013). Cates and Mojzsis (2007) also established a firm minimum age for the sequence at 3.75 Ga from a trondhjemitic sheet crosscutting amphibolites and BIF near the southern tip of the belt. The geochronological implications of these results depend on the nature of zircon-bearing protoliths, as well as their field relationship with the cummingtonite-amphibolite unit, the contentious nature of which has produced diverging interpretations of the zircon record (Augland and David, 2015; Darling et al., 2013). Nevertheless, the picture that emerges from conventional geochronological approaches points towards an Eoarchean age for the NSB, in contrast to the ca. 4.3 Ga date provided by the ^{146}Sm – ^{142}Nd system. Hence, while the isotopic signal carried by Nuvvuagittuq rocks is exceptional – and may hold the key to a better understanding of the Hadean geological evolution – the fundamentals of both its chronological and geodynamic significance remain unclear.

The geochronological issue raised by the NSB ^{146}Sm – ^{142}Nd record is further exacerbated by the poor preservation of the mafic lithologies carrying the ^{142}Nd anomalies (O'Neil et al., 2011). This is due to hydrothermal and metamorphic processes (e.g. Cates and Mojzsis, 2009) which resulted in severe disturbance of their geochemical signatures and currently prevents reliable dating using conventional radiogenic isotope systems (Guitreau et al., 2013; O'Neil et al., 2012; Roth et al., 2013; Touboul et al., 2014). The Nuvvuagittuq belt, however, is not the singular occurrence of supracrustal rocks in the wider Innuksuac complex; regional mapping, aerial photographs and aeromagnetic surveys also show the presence of a dozen or so scattered supracrustal enclaves in the general area of the Inukjuak domain (Simard et al., 2003), none

of which have previously been subject to any detailed field or geochronological investigation. Here, we present high-precision $^{146,147}\text{Sm}$ – $^{142,143}\text{Nd}$ data for a mapped unit of magmatic and sedimentary rocks from the Ukaliq¹ supracrustal belt (USB), a newly discovered volcano-sedimentary enclave situated a few kilometers north of the NSB. Our results show that mafic lithologies of the USB define a rough positive correlation between $^{142}\text{Nd}/^{144}\text{Nd}$ and Sm/Nd , which, if interpreted as an isochron, would yield a Hadean emplacement age similar to that reported for Nuvvuagittuq. Our observations, however, consistently point towards an inherited origin for the ^{142}Nd effects. We show how this vestigial signal in turn provides a means to better understand the geodynamic evolution of the young Earth, from the crystallization of the magma ocean to the genesis of the oldest continental nuclei.

2. Geological setting

The Ukaliq supracrustal belt (USB) belongs to one of several scattered enclaves of the Innuksuac complex, a group of plutonic and supracrustal rocks rafted within the predominantly Neoproterozoic Inukjuak domain (Minto block, Northeast Superior Province (NESP), Quebec). The geology of the region has been described in detail in several previous studies (e.g. Cates and Mojzsis, 2007, 2009; Cates et al., 2013; Stevenson et al., 2006; O'Neil et al., 2007) and we only focus here on the newly discovered Ukaliq outcrops. The Ukaliq enclave (Fig. 1) is composed of interleaved rocks of volcanic and sedimentary protolith that are intruded by late leucogranitoids and surrounded by 3.45–3.65 Ga tonalitic gneisses of the Voizel suite. Located approximately 5–10 km north of Nuvvuagittuq, the USB is an asymmetrical belt with a maximum thickness of 60 m and a NNW-trending extent of several kilometers. Its southernmost exposure – the focus of this study – is within a low-strain window dominated by amphibolites (*Am*) and variably serpentinized ultramafic rocks (*Aum*), with minor sedimentary components including iron formations (*BIF*), quartzite (*Aq*) and quartz–biotite schists (*Aqbc*) of probable detrital sedimentary origin. Although the Ukaliq enclave is largely intact, the sequence has been strongly deformed, transposed, and like the rest of the Inukjuak domain was metamorphosed to the upper amphibolite facies (Cates and Mojzsis, 2009). The ultramafic units show clear evidence at the outcrop scale for extensive alteration, and range from pure serpentinites on the eastern side of the sequence to more pyroxene-rich compositions toward the West. We interpret this field relation to reflect a relict magmatic differentiation trend within a komatiitic flow. The presence of chemical sediments near to what we interpret to be the base of the sequence points to a predominantly volcanic or subvolcanic origin for the mafic/ultramafic rocks. It is noteworthy that unlike in the NSB, cumingtonite-rich amphibolites rarely occur in the USB. We interpret this to reflect the absence of the hydrothermally altered, low-Ca mafic lithologies that volumetrically dominate in the Nuvvuagittuq belt.

Our sample set was collected in the mapped exposures on the southern part of the USB during fieldwork in 2012 and 2014. The collection consists of 38 amphibolites and ultramafic rocks, 6 chemical sediments, 13 granitoid gneisses (Voizel suite), and 2 Neoproterozoic granites (Boizard suite) sampled from the enclosing gneisses of the supracrustals. Sample locations are reported on the map (Fig. 1), and correlated GPS coordinates are provided in Appendix A1.

3. Whole-rock geochemistry

3.1. Mafic and ultramafic rocks

Whole-rock major and trace element analyses were performed on amphibolites and ultramafic rocks representative of the main lithological units of the USB (Appendix A1). Most Ukaliq ultramafic rocks are distinguished by high Al/Ti and low Gd/Yb ratios and, overall, are compositionally similar to Al-enriched komatiites (Appendix A1) (Arndt et al., 2008). Their high degree of serpentinization and metasomatism expected to occur during hydrothermal alteration renders these rocks poorly suited for ^{147}Sm – ^{143}Nd studies. Thus, with the exception of one relatively well preserved pyroxenite, and two hornblendites sampled near the top of the main ultramafic body, this category of rock samples is not further considered in this study.

Mafic lithologies of the USB display a wide compositional range, with $\text{SiO}_2 = 46$ – 53 wt%, $\text{MgO} = 7$ – 12 wt% and $\text{CaO} = 4$ – 12 wt% (Fig. 2, Appendix A2). Most samples define a trend of decreasing incompatible elements (e.g. ΣREE) with increasing SiO_2 content (Fig. 2), which cannot be described as a magmatic differentiation trend and suggests the presence of distinct primary magma compositions. The major and trace element characteristics, in conjunction with petrographic examination of thin sections, contribute to distinguishing four subtypes of mafic rocks within this outcrop, hereafter referred to as *tholeiitic*, *transitional*, *boninitic* and *enriched*. The main characteristics of these four groups are illustrated in plots of Al/Ti versus selected major and trace elements in Fig. 2, and can be summarized as follows:

Tholeiitic lavas ($N = 9$) have low SiO_2 content (46–49 wt%) and $\text{Al}_2\text{O}_3/\text{TiO}_2$ ratios ranging from 10 to 20. With the exception of one specimen with anomalously high SiO_2 , this group is fairly homogeneous, with $\text{CaO} \approx 10$ wt%, $\text{MgO} \approx 8$ wt%, $\text{Al}_2\text{O}_3 \approx 15$ wt% and $\text{Fe}_2\text{O}_3 \approx 12$ – 15 wt%. Despite low silica contents, samples show the highest overall abundance of incompatible elements, with $\Sigma\text{REE} = 25$ – 60 ppm and $\text{TiO}_2 = 0.7$ – 1.3 wt%, consistent with derivation of their parent magma from a relatively fertile mantle source. Samples from this group have flat chondrite-normalized REE patterns (Appendix A2), exhibit a slight depletion in LILE and show little or no HFSE anomaly.

Boninitic lavas ($N = 5$), in contrast, have markedly higher SiO_2 content (50–53 wt%) and $\text{Al}_2\text{O}_3/\text{TiO}_2$ ratios (27–30) associated with low CaO (5 wt%) and high MgO (12 wt%) contents. This group has the lowest overall abundance of incompatible elements ($\Sigma\text{REE} = 20$ – 30 ppm, $\text{TiO}_2 = 0.5$ wt%), is markedly enriched in Cr (up to 800 ppm), and exhibits a concave upward trace element pattern with sub-chondritic $(\text{Gd}/\text{Yb})_N$ and superchondritic $(\text{La}/\text{Sm})_N = 1.5$ – 1.9 . Trace element patterns show pronounced negative Nb–Ta anomalies $((\text{Nb}/\text{Th})_N \approx 0.3)$, and slight excesses of Zr compared to the adjacent REE. The major and trace element characteristics of this group are reminiscent of modern low-Ca boninites (Crawford et al., 1989), although only 2 out of 5 samples have SiO_2 contents high enough to classify as *sensu stricto* boninites according to the IUGS nomenclature (Le Bas, 2000).

Intermediate between tholeiitic and boninitic lavas, the *'transitional'* group ($N = 5$) is characterized by $\text{Al}_2\text{O}_3/\text{TiO}_2$ ratio typically ranging between 20 and 25, and SiO_2 content between 48 and 50 wt%. Samples from this group exhibit low Nb/Th and high Th/Yb ratios similar to the boninitic lavas, and their major element composition is essentially identical to the tholeiitic group, albeit with lower TiO_2 (and ΣREE) contents suggestive of a more refractory mantle source.

Lastly, a single specimen (IN12032), hereafter referred to as *enriched metabasalt*, is characterized by high SiO_2 (52 wt%), together with high REE content ($\Sigma\text{REE} = 52$ ppm), and a marked enrichment in LILE $((\text{Th}/\text{Yb})_N = 5.9)$. The sample displays negative

¹ Ukaliq (ᐃᐅᐅᐅᐅ) is “Arctic hare” *Lepus arcticus* in the local Inuktitut language of Nunavik in northern Québec, and is used by us as an informal field name for this supracrustal enclave.

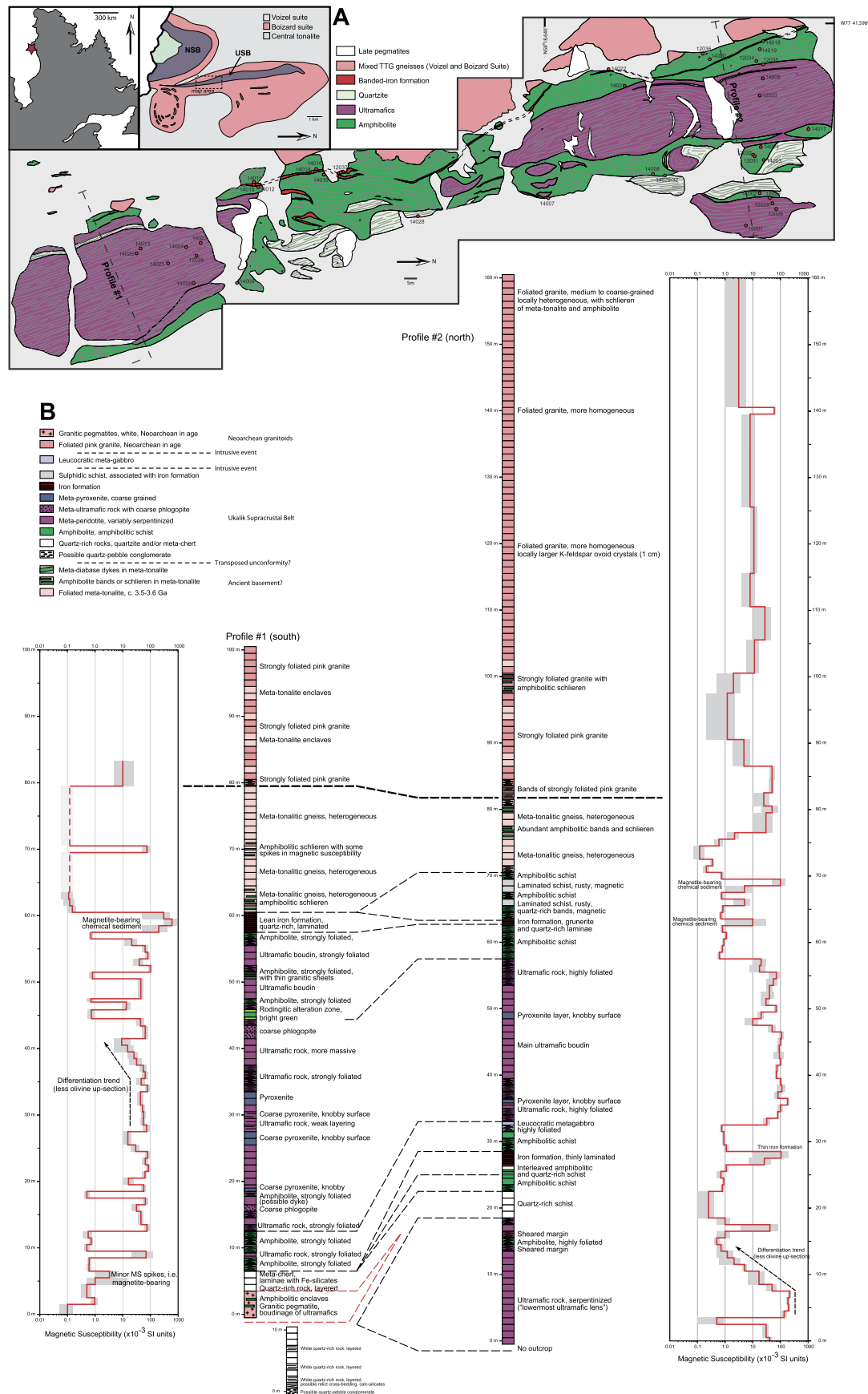


Fig. 1. (A) Geographical location and geological map of the southern part of the Ukalik supracrustal belt showing the main lithological units and sampling sites. GPS coordinates for samples analyzed in this study are provided in the electronic supplement. (B) Lithological sections and magnetic susceptibility profiles across the Ukalik belt. (For interpretation of the colors in this figure, the reader is referred to the web version of this article.)

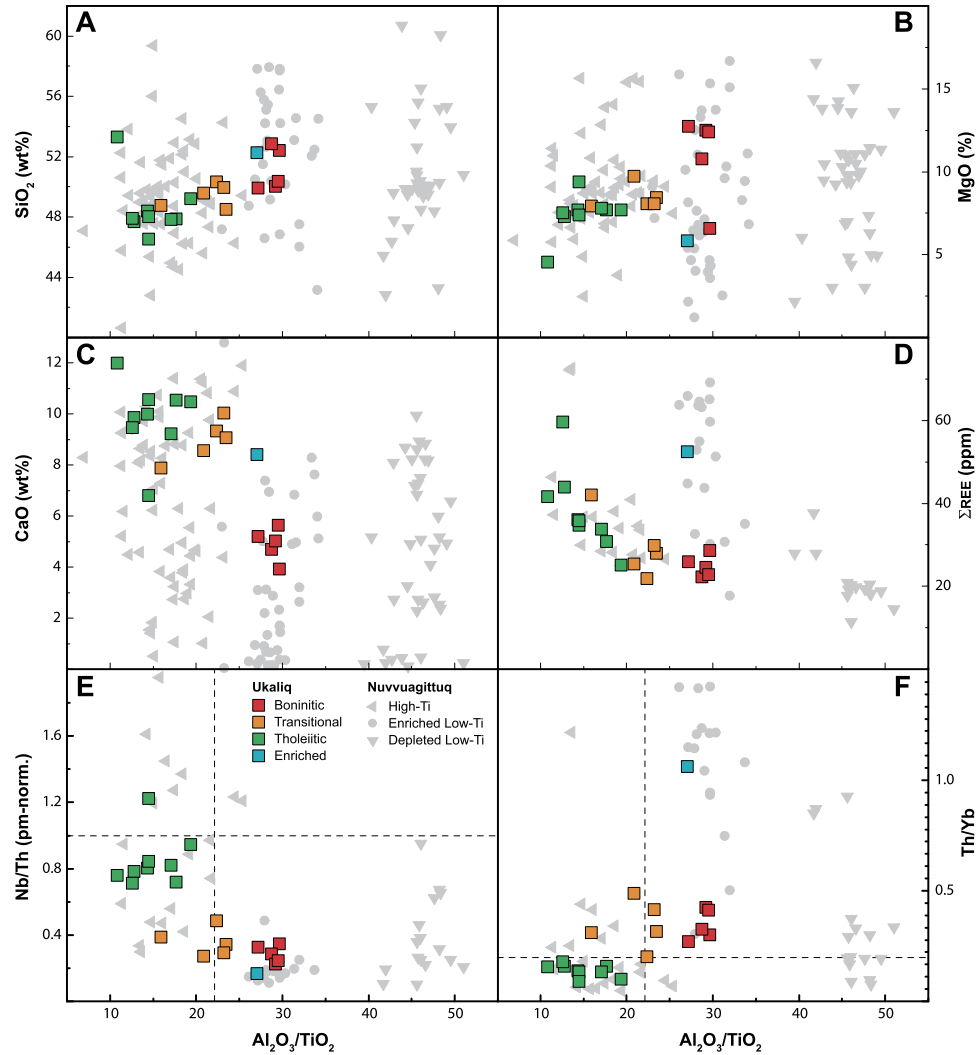


Fig. 2. $\text{Al}_2\text{O}_3/\text{TiO}_2$ vs selected major and trace element in mafic lavas of the Ukalik and Nuvvuagittuq supracrustal belts. Data for the Ukalik belt are available in electronic supplement. Nuvvuagittuq data are compiled from the literature (Cates and Mojzsis, 2007; Cates et al., 2013; O'Neil et al., 2007, 2008, 2011). (For interpretation of the colors in this figure, the reader is referred to the web version of this article.)

Nb and Ti anomalies reminiscent of magmas from modern calc-alkaline series, although its FeO/MgO ratio of 1.6 does not place it unambiguously within the calc-alkaline field of the Miyashiro diagram. As will be discussed later (section 5), the major and trace element chemistry of this sample points either towards assimilation of a tonalitic contaminant at crustal level, or metasomatic enrichment of a depleted mantle source by tonalitic melts.

Overall, the geochemistry of Ukalik amphibolites closely resembles that described for “metabasalts” in Nuvvuagittuq. Tholeiitic and transitional amphibolites from our outcrops would fall into what has been termed in the NSB as the “High-Ti” group, while the enriched and boninitic lavas are similar to the “enriched low-Ti” and “depleted low-Ti” groups, respectively (O'Neil et al., 2011). Ukalik lavas, therefore, appear to bear some relation to the cummingtonite–amphibolites at Nuvvuagittuq. They nevertheless display less compositional heterogeneity, most likely reflecting a different alteration history, than their respective equivalents in the NSB. Specifically, the exposed lithologies show no evidence for secondary loss of Ca and Na (Fig. 2C), suggesting that the hydrothermal event proposed to have mobilized all but the most immobile elements in NSB mafic protoliths (Cates et al., 2013) did not affect the Ukalik rocks. While our USB samples show local evidence for secondary silicification and metasomatism, they define coherent compositional fields, which we conclude are more likely than

the highly altered NSB cummingtonite–amphibolites to reflect primary characteristics of their parent magmas.

3.2. Chemical sediments (Quartzites and BIFs)

Magnetite-bearing rocks of chemical sedimentary origin occur both on the eastern side of the sequence, as a discontinuous Si-rich layer locally grading into cherty units, and on the western side, as a nearly continuous 50 cm–1 m wide Fe-rich layer of probable BIF protolith interleaved with mafic rocks (Fig. 1). The specimen sampled on the eastern side has high SiO_2 content (89 wt%) and low Fe_2O_3 (8.5 wt%), with all other oxides below or equal to 1 wt%. BIFs sampled on the western side have high Fe_2O_3 contents (35–70 wt%), $\text{MgO} = 4\text{--}7$ wt% and $\text{Al}_2\text{O}_3 = 0.6\text{--}2$ wt%. All samples display shale-normalized REE + Y patterns typical of Archean marine sediments, marked by a depletion of LREE compared to HREE, small positive Eu anomalies and elevated Y/Ho ratios (Fig. 3).

4. Results

$^{146,147}\text{Sm}\text{--}^{142,143}\text{Nd}$ results for 21 amphibolites, 2 hornblendites, 1 pyroxenite, 14 granitoid gneisses and 11 chemical sediments of the Ukalik belt and surrounding Innuksuac complex are summarized in Table 1 and Fig. 4. Individual analyses for sam-

Table 1
 $^{146,147}\text{Sm}$ – $^{142,143}\text{Nd}$ results for volcanic, plutonic and sedimentary rocks of the Ukalik belt and Innuvuagittuq complex.

Sample	Lithology/Group	U–Pb age (Ma)	^{144}Nd (nM/g)	[Nd] (ppm)	^{147}Sm (nM/g)	[Sm] (ppm)	$^{147}\text{Sm}/^{144}\text{Nd}$	$^{143}\text{Nd}/^{144}\text{Nd}$	\pm (2 S.E.) (10^{-6})	$\varepsilon^{143}\text{Nd}_i^a$	T_{DM} (Ga)	$\mu^{142}\text{Nd}$	\pm (2 S.E.)
IN14004	Am/Tholeiitic		13.1	7.95	2.69	2.70	0.2049	0.512818	3.56	−0.6	8.7	−3.2	0.5
IN14012	Am/Tholeiitic		13.6	8.23	2.67	2.68	0.1965	0.512675	3.44	0.6	4.0	−3.4	3.4
IN14016	Am/Tholeiitic		11.4	6.90	2.28	2.29	0.2003	0.512765	3.16	0.6	4.2	−1.3	3.1
IN14022	Am/Tholeiitic		10.9	6.63	2.20	2.21	0.2011	0.512777	3.22	0.4	4.5	−2.0	2.9
IN14019	Am/Tholeiitic		7.91	4.80	1.65	1.66	0.2089	0.512951	2.60	0.0	−1.0	−1.3	1.7
IN14009	Am/Tholeiitic		11.5	6.94	2.28	2.29	0.1990	0.512711	7.77	0.1	4.6	0.1	1.7
IN12015	Am/Tholeiitic		10.1	6.15	1.96	1.96	0.1928	0.512633	2.87	1.6	3.4	−0.3	0.7
IN12018	Am/Tholeiitic		9.23	5.59	1.81	1.81	0.1960	0.512668	3.11	0.7	3.9	0.6	3.0
IN14002	Am/Tholeiitic		19.8	12.00	3.39	3.40	0.1771	0.512240	3.67	1.6	3.6	−0.5	2.2
IN14003	Am/Trans.		11.9	7.23	2.14	2.15	0.1794	0.512293	2.78	1.5	3.6	−4.0	2.9
IN12013	Am/Trans.		8.46	5.13	1.56	1.57	0.1847	0.512353	6.02	0.1	4.1	−3.9	0.8
IN14007	Am/Trans.		8.50	5.15	1.62	1.63	0.1906	0.512503	2.91	0.1	4.2	−3.9	3.6
IN14015	Am/Trans.		6.52	3.95	1.26	1.26	0.1931	0.512518	3.21	−0.8	4.7	−5.2	3.8
IN14017	Am/Trans.		7.57	4.59	1.49	1.49	0.1964	0.512619	2.95	−0.4	4.7	−3.2	4.5
IN14032	Am/Boninitic		7.38	4.48	1.26	1.26	0.1700	0.512016	3.51	0.6	3.8	−4.5	3.0
IN14029	Am/Boninitic		5.62	3.41	1.04	1.04	0.1841	0.512259	4.01	−1.5	4.6	−3.7	3.1
IN14006	Am/Boninitic		7.00	4.24	1.29	1.29	0.1844	0.512319	2.60	−0.5	4.2	−3.8	3.2
IN12031	Am/Boninitic		6.66	4.04	1.20	1.20	0.1789	0.512097	5.61	−2.1	4.6	−3.4	3.6
IN12034	Am/Boninitic		6.31	3.83	1.11	1.11	0.1754	0.512101	6.72	−0.3	4.1	−5.4	1.6
IN12032	Am/Enriched		15.6	9.44	2.35	2.36	0.1507	0.511399	3.45	−2.1	4.2	−9.4	2.8
IN14020	Aum		22.5	13.63	3.98	4.00	0.1771	0.512181	4.22	0.4	3.9	−1.0	0.4
IN12036	Aum		13.0	7.90	2.67	2.68	0.2053	0.512875	4.08	0.3	6.5	−0.6	0.5
IN14011	Aum		5.34	3.24	1.02	1.02	0.1906	0.512444	3.10	−1.0	4.7	−0.9	3.5
IN12012	TTG	3652	40.6	24.61	4.37	4.38	0.1076	0.510387	2.70	−2.6	3.90	−5.1	1.3
IN12041	TTG	3550	27.2	16.46	3.03	3.04	0.1117	0.510589	4.06	−1.7	3.75	0.8	3.5
IN12014	TTG	3550	44.5	26.97	3.36	3.37	0.0756	0.510088	1.96	5.1	3.30	−7.7	2.8
IN12017	TTG	3598	21.8	13.22	2.26	2.27	0.1038	0.510387	3.28	−1.4	3.76	−5.5	3.7
IN12053	TTG	3412	23.2	14.04	2.82	2.83	0.1217	0.510976	3.35	0.0	3.51	−3.9	3.2
IN12042	TTG	3492	24.7	15.00	2.00	2.01	0.0809	0.509852	3.22	−2.8	3.72	−3.9	4.6
IN12027	TTG	3519	12.5	7.59	1.50	1.50	0.1197	0.510725	2.84	−3.0	3.85	−5.4	1.8
IN12046	TTG	3483	44.9	27.23	3.89	3.91	0.0867	0.510144	2.08	0.1	3.53	−8.2	4.0
IN12050	TTG	3437	20.6	12.46	1.66	1.66	0.0807	0.510000	2.23	−0.7	3.54	−4.7	5.1
IN12016	Granite	2706	24.5	14.83	3.38	3.39	0.1381	0.511352	3.63	−5.3	3.52	−1.5	3.1
IN12054	Granite	2720	93.8	56.83	5.95	5.97	0.0635	0.510030	2.61	−4.9	3.09	0.7	3.3
IN12037	BIF (Ukalik)		7.76	4.702	1.21	1.216	0.1562	0.511585	4.30	−2.4	4.07	−2.8	3.2
IN14010	BIF (Ukalik)		7.35	4.453	1.07	1.070	0.1452	0.511408	2.86	0.8	3.78		
IN14014	BIF (Ukalik)		11.6	7.011	1.75	1.754	0.1512	0.511465	3.18	−1.0	4.03	−2.4	2.1
IN14018	BIF (Ukalik)		12.4	7.545	1.87	1.881	0.1506	0.511528	3.76	0.5	3.82		
IN14027	BIF (Ukalik)		1.01	0.612	0.15	0.150	0.1480	0.511305	4.78	−2.6	4.21	−1.8	3.7
IN14028	BIF (Ukalik)		74.7	0.453	0.10	0.105	0.1399	0.511497	3.24	5.1	3.29	−0.4	3.3
IN08030	BIF (Nuvvuagittuq)		0.94	0.572	0.20	0.205	0.2165	0.512676	3.67	−8.9	−4.81	−3.7	3.2
IN05007	BIF (Nuvvuagittuq)		2.21	1.340	0.33	0.332	0.1497	0.511696	3.12	4.4	3.33	−2.4	3.0
IN05010	BIF (Nuvvuagittuq)		2.76	1.674	0.37	0.372	0.1344	0.511273	2.96	3.6	3.50	−2.6	1.0
IN08026	BIF (Nuvvuagittuq)		3.30	2.003	0.50	0.505	0.1524	0.511500	2.74	−0.8	4.02	−2.4	3.1
IN08032	BIF (Nuvvuagittuq)		0.44	0.269	0.10	0.106	0.2387	0.513218	6.72	−9.1	1.24		
GR04-20	BIF (Isua)		1.71	1.039	0.20	0.198	0.1151	0.511042	3.20	7.6	3.15	−4.1	4.2
IFG	BIF (Isua)		2.66	1.615	0.37	0.376	0.1405	0.511311	2.65	0.6	3.73	−1.6	1.4
GR04-048	BIF (Isua)		2.47	1.497	0.31	0.311	0.1256	0.511010	3.33	1.9	3.61	−1.5	3.7

^a Initial $\varepsilon^{143}\text{Nd}$ are calculated assuming a deposition age of 3.75 Ga for the Ukalik and Nuvvuagittuq BIFs and volcanic rocks, and 3.7 Ga for Isua samples.

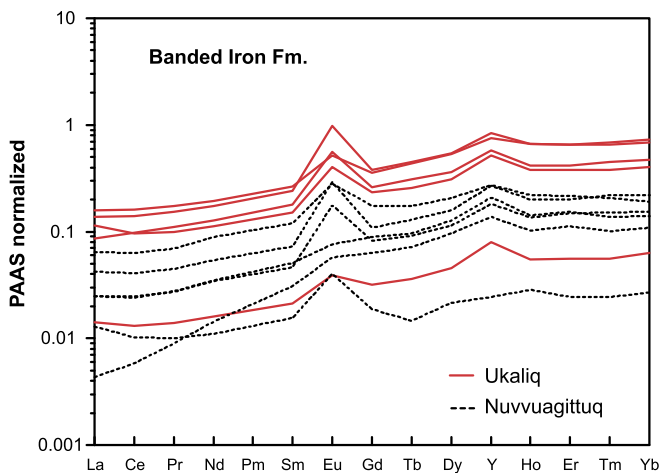


Fig. 3. Shale-normalized REE + Y patterns for Ukalik and Nuvvuagittuq BIFs analyzed in this study. PAAS: Post-Archean Australian Shale. (For interpretation of the colors in this figure, the reader is referred to the web version of this article.)

ples and standards, as well as analytical methods employed for ^{147}Sm – ^{143}Nd and ^{142}Nd analyses are provided in Appendices A3–A4. Reproducibility of the JNdi standard during the course of this study was on average of ± 3 ppm (2 S.D.) (Appendix A3). Variations of the $^{142}\text{Nd}/^{144}\text{Nd}$ ratio, noted as $\mu^{142}\text{Nd}$, are expressed as relative deviations (in ppm) with regards to the JNdi standard. Variations of the $^{143}\text{Nd}/^{144}\text{Nd}$ ratio are expressed using the conventional ε notation, after normalization to the CHUR value (Bouvier et al., 2008). Throughout the paper, ^{146}Sm – ^{142}Nd ages are calculated using an initial $^{146}\text{Sm}/^{144}\text{Sm}$ ratio of 0.0082 and a half-life of 103 Ma (Meissner et al., 1987; Marks et al., 2014). Alternative ages calculated using a half-life of 68 Ma for ^{146}Sm (Kinoshita et al., 2012) are also provided in parenthesis, in which case the initial $^{146}\text{Sm}/^{144}\text{Sm}$ ratio was adjusted to 0.0094. Unless stated otherwise, errors are quoted as 2 standard deviations (S.D.).

4.1. Amphibolites and ultramafic rocks

As shown in Fig. 4, each group of mafic/ultramafic rocks is characterized by a distinct and internally homogeneous ^{142}Nd sig-

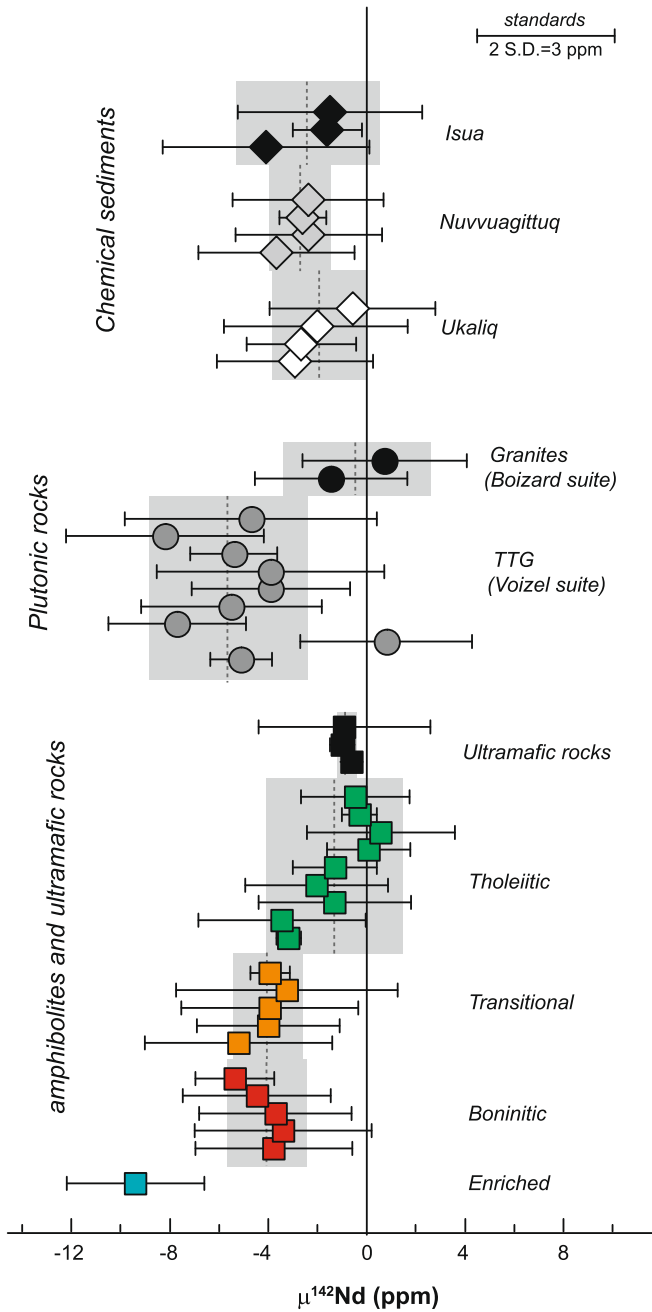


Fig. 4. Summary of ^{142}Nd results for volcanic rocks, plutonic rocks and chemical sediments analyzed in this study. Errors for individual analyses (or individual samples) are given as 2 S.E. Grey fields represent 2 S.D. errors on averages obtained for each lithologic type or location. (For interpretation of the colors in this figure, the reader is referred to the web version of this article.)

nature. Tholeiitic and ultramafic lavas have $\mu^{142}\text{Nd}$ within error of the modern mantle value, at -1.3 ± 2.8 ppm and -0.8 ± 0.4 ppm, respectively. In contrast, the boninitic and transitional lavas exhibit similar negative effects at -4.1 ± 1.6 ppm and -4.7 ± 2.8 ppm. Lastly, the enriched amphibolite (IN12032) exhibits the lowest $\mu^{142}\text{Nd}$ signature at -9.4 ± 3 ppm. When plotted in a $^{142}\text{Nd}/^{144}\text{Nd}$ vs Sm/Nd space (Fig. 5A), mafic rocks define a rough positive correlation which, if considered as an isochron relationship, yields an apparent emplacement age of 4215^{+50}_{-76} Ma (or 4321^{+33}_{-50} Ma using $T_{1/2} = 68$ Ma). This result is similar to that obtained from mafic samples of the NSB (O'Neil et al., 2008; Roth et al., 2013), confirming the close relationship between Ukalik and Nuvvuagittuq.

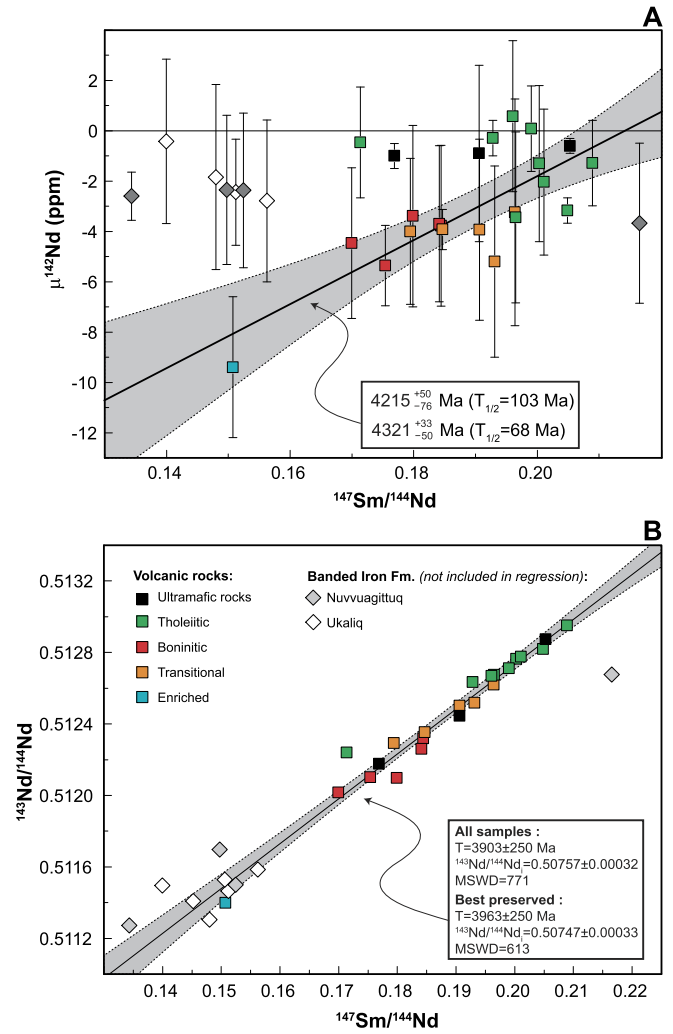


Fig. 5. (A) ^{146}Sm – ^{142}Nd results for volcanic and sedimentary rocks of the Ukalik and Nuvvuagittuq belts, plotted in a conventional isochron diagram. The gray field represents the 2 S.D. error envelope for the regression on mafic lavas (Sample IN14002 is excluded from regression). (B) ^{147}Sm – ^{143}Nd errorchron obtained on volcanic rocks of the Ukalik belt. Both regressions are calculated using Isoplot (Ludwig, 1991). (For interpretation of the colors in this figure, the reader is referred to the web version of this article.)

The ^{147}Sm – ^{143}Nd results obtained from Ukalik lavas (Fig. 5B) show substantial excess scatter and, overall, provide an imprecise date of 3903 ± 250 Ma. Eliminating samples showing signs of secondary alteration, silicification or K-metasomatism results in a slightly older age estimate at 3963 ± 250 Ma. As for the ^{146}Sm – ^{142}Nd array, the slope of the ^{147}Sm – ^{143}Nd errorchron is largely controlled by the enriched amphibolite; disregarding this sample yields a younger age of 3735 ± 320 Ma that resembles U–Pb zircon geochronology for the oldest gneissic components of the NSB (Cates and Mojzsis, 2007). Regressions obtained by pooling together samples with identical $\mu^{142}\text{Nd}$ yield imprecise but similar Eoarchean dates at 3588 ± 410 Ma (tholeiitic and ultramafics) and 3677 ± 480 Ma (transitional and boninitic). Hence, the ^{147}Sm – ^{143}Nd systematics do not substantiate a Hadean emplacement age for Ukalik lavas.

4.2. Plutonic rocks

Tonalitic gneisses sampled in the vicinity of Ukalik have zircon U–Pb ages ranging from 3.45 Ga to 3.65 Ga, and ^{147}Sm – ^{143}Nd model ages (T_{dm}) ranging from 3.3 to 3.9 Ga. With the exception of IN12014, all TTG gneisses have negative $\varepsilon^{143}\text{Nd}_i$ ranging from

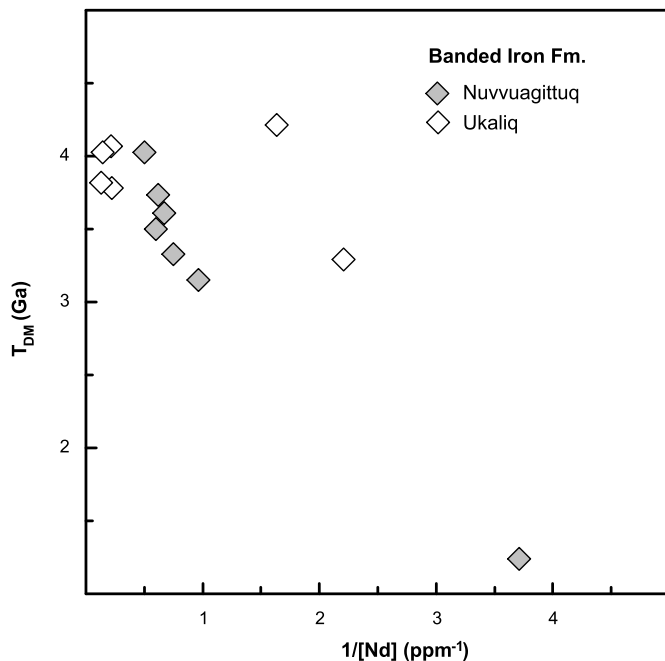


Fig. 6. Depleted Mantle model ages (T_{DM}) for BIFs of the Ukalik and Nuvvuagittuq belts. Note that most samples show a trend of decreasing model ages with decreasing Nd content, consistent with open system behavior during late metamorphic events. Samples with high Nd abundances from the Ukalik belt define a narrower age range, consistent with closed-system behavior since 3.8–4 Ga.

0 to -3 , and all but one sample have negative $\mu^{142}\text{Nd}$ averaging -5.6 ± 3.2 ppm. On the other hand, Neoarchean granites have $\mu^{142}\text{Nd}$ within error of the modern terrestrial value, despite negative $\varepsilon^{143}\text{Nd}_i$ indicative of a crustal precursor. These results confirm the presence of an inherited Hadean component in the Voizel suite, as previously reported by O'Neil et al. (2008) and Roth et al. (2013). This Hadean component, however, does not appear to have been involved in later magmatic events in the area.

4.3. Rocks of chemical sedimentary origin

New $^{146,147}\text{Sm}$ – $^{142,143}\text{Nd}$ analyses for magnetite-bearing rocks of probable BIF protolith from the Nuvvuagittuq, Ukalik and Isua supracrustal belts are summarized in Fig. 4. Nuvvuagittuq BIFs define an imprecise date of 2719 ± 610 Ma, similar to a two-point isochron age, suggesting at least partial isotopic equilibration on a whole-rock scale during metamorphism associated with assembly of NESP terranes in the Neoarchean (Cates and Mojzsis, 2009). Disturbance of the ^{147}Sm – ^{143}Nd chronometer in NSB samples with low Nd contents is also evidenced by highly scattered model ages (Fig. 6) which prevents determination of a deposition age using this method. From another standpoint, four USB samples with markedly higher Nd contents yield homogeneous model ages at 3.78–4.07 Ga, similar to the ^{147}Sm – ^{143}Nd age derived from mafic/ultramafic samples. Despite variably disturbed ^{147}Sm – ^{143}Nd systematics, all samples from Ukalik and Nuvvuagittuq present identical $\mu^{142}\text{Nd}$ within errors of the terrestrial value, at -1.9 ± 2.1 and -2.7 ± 1.3 ppm, respectively. As shown in Fig. 5A, BIFs from Ukalik and Nuvvuagittuq do not plot on the ^{146}Sm – ^{142}Nd array defined by volcanic rocks. Their $\mu^{142}\text{Nd}$ is constant, irrespective of their Sm/Nd ratio, and identical to that inferred for the Eoarchean ocean from our analyses of Isua BIFs ($\mu^{142}\text{Nd} = -2.4 \pm 3$ ppm). Thus, despite their stratigraphic relationships with mafic lavas carrying the ^{142}Nd anomalies, chemical sediments in the Ukalik/Nuvvuagittuq belts show no evidence for in situ decay of ^{146}Sm that would be expected from a Hadean deposition age.

5. Discussion

5.1. Radiogenic vs. inherited ^{142}Nd anomalies

The apparent ^{146}Sm – ^{142}Nd and ^{147}Sm – ^{143}Nd ages derived from magmatic rocks of the USB, while somewhat less discordant than those obtained for Nuvvuagittuq, remain subject to the same ambiguities raised by previous investigations of the NSB. Since magmas derived from sources with different $\mu^{142}\text{Nd}$ would also have distinct initial $^{143}\text{Nd}/^{144}\text{Nd}$ ratios, all ^{147}Sm – ^{143}Nd ages obtained from Ukalik and Nuvvuagittuq lavas are inherently problematic. Contamination of Eoarchean magmas by a Hadean enriched component would, in fact, generate mixing lines with positive slopes in both the ^{146}Sm – ^{142}Nd and ^{147}Sm – ^{143}Nd isochron plots. Therefore, even the near-concordant Hadean dates derived from filtered subsets of mafic rocks by O'Neil et al. (2012) are ambiguous, consistent either with a Hadean emplacement age or the presence of an inherited component within younger lavas. The geochronological significance of any Sm–Nd results for these rocks is further obscured by the fact that the major and trace element variability observed in mafic lavas, and therefore most of the observed spread in Sm/Nd, is not primarily controlled by magmatic differentiation but most likely by source heterogeneities (Section 5.3). These observations preclude a straightforward age determination from either the ^{146}Sm – ^{142}Nd or ^{147}Sm – ^{143}Nd chronometers. Examination of the fine structure of the $^{142,143}\text{Nd}$ signal, however, reveals several key features that consistently point towards an inherited origin for the negative anomalies in Ukalik lavas. First, ^{147}Sm – ^{143}Nd regressions obtained by pooling samples with identical $^{142}\text{Nd}/^{144}\text{Nd}$ (and, arguably, identical initial $^{143}\text{Nd}/^{144}\text{Nd}$), yield imprecise but clearly younger ages than that obtained from the ^{146}Sm – ^{142}Nd array (Section 4.1). Second, the presence of ^{142}Nd anomalies appears to be mainly restricted to lavas with boninitic affinities, suggesting derivation from a metasomatically enriched mantle source (section 5.3). In contrast, tholeiitic and ultramafic rocks have constant $\mu^{142}\text{Nd}$ irrespective of their Sm/Nd ratio (Fig. 5A). Lastly, our results on chemical sediments of the USB and NSB are difficult to reconcile with a Hadean emplacement age. BIFs have low Sm/Nd ratios that reflect on the predominantly crustal origin of REE in seawater (e.g. Mloszewski et al., 2013), so that deposition before 4.1 Gyr ago is expected to have resulted in the production of significant ^{142}Nd anomalies (typically -10 ppm for a 4.25 Ga deposition age). The BIFs of the USB and NSB, however, show no statistically resolvable effect. Their $\mu^{142}\text{Nd}$ is indistinguishable from the signature of Eoarchean seawater, as inferred from the Isua BIFs analyses. We conclude that this observation is inconsistent with deposition of BIF protoliths at a time when ^{146}Sm was still extant.

The lack of ^{142}Nd anomalies in chemical sediments of the Ukalik/Nuvvuagittuq belts has implications for the geochronology of supracrustal enclaves in the Innuksuac complex. Chemical sediments in both belts are stratigraphically interleaved with mafic lavas carrying variable ^{142}Nd anomalies (Mloszewski et al., 2012; O'Neil et al., 2011). Further, field observations revealed no evidence for tectonic intercalation of the BIFs within the associated mafic/ultramafic sequences. Hence, the lack of unradiogenic effects despite low Sm/Nd ratios characterizing these lithologies cannot be explained by late sedimentation on a pre-existing Hadean mafic crust. While samples with low Nd content show evidence for late disturbance of the ^{147}Sm – ^{143}Nd system, the Ukalik BIFs with high Nd content yield Eoarchean model ages consistent with U–Pb zircon geochronology, and show no compelling evidence for isotopic resetting during Neoarchean metamorphism. Thus, while it is difficult to entirely disprove the possibility of open system behavior of the ^{146}Sm – ^{142}Nd system in BIFs, we believe that the similarity between Isua, Ukalik and Nuvvuagittuq samples is more than mere coincidence. The most plausible interpretation is that chemical

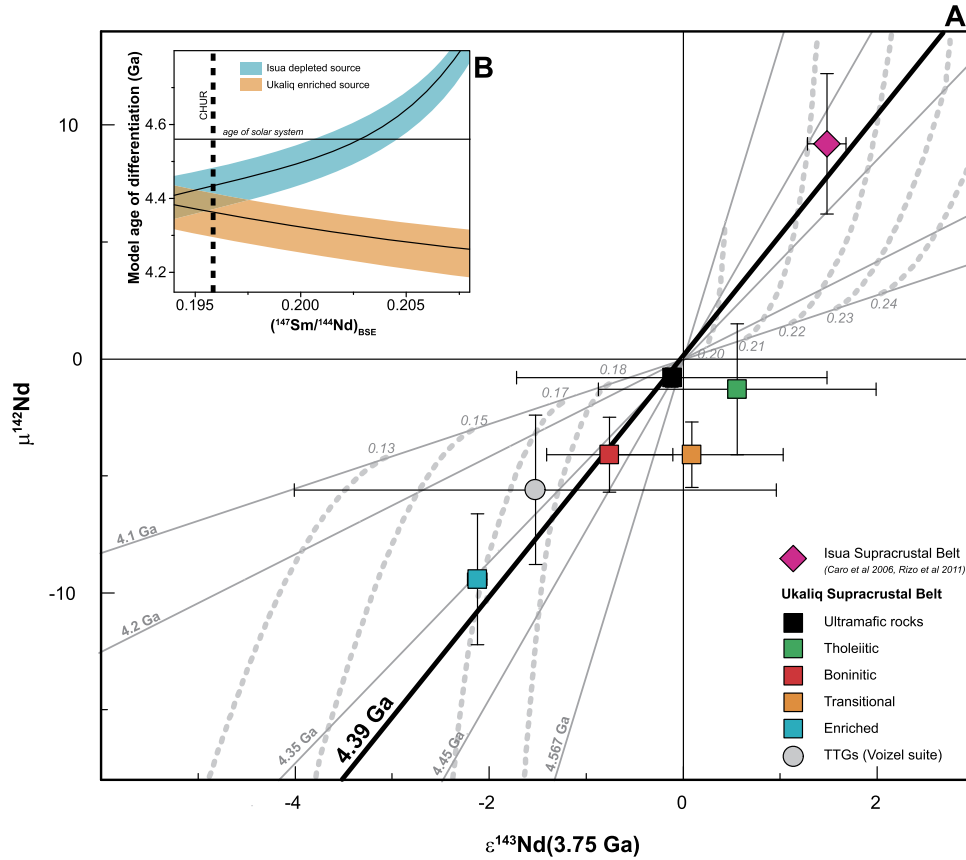


Fig. 7. (A) Coupled $^{146,147}\text{Sm}$ – $^{142,143}\text{Nd}$ systematics for magmatic rocks of the Ukalik belt and surrounding TTGs of the Voizel suite. The $^{142,143}\text{Nd}$ systematics of Isua supracrustal belt (3.7–3.8 Ga; Caro et al., 2006) are shown for comparison. The dashed curves represent loci of constant $(^{147}\text{Sm}/^{144}\text{Nd})_{\text{source}}$ ratios, ranging from 0.13 to 0.24, in the Hadean source. Solid lines are loci of constant model ages, ranging from 4.1 Ga to 4.567 Ga. The thick black line represents a linear regression including Isua and Ukalik data. (B) Dependence of the calculated model ages for Isua and Ukalik sources on the BSE Sm/Nd ratio. All ages are calculated using a half-life of 103 Ma for ^{146}Sm . Ages calculated using a half-life of 68 Ma are provided in the text. (For interpretation of the colors in this figure, the reader is referred to the web version of this article.)

sediments that are found interleaved within the Ukalik/Nuvvuagittuq sequences deposited at a time when ^{146}Sm was extinct, from an Eoarchean ocean isotopically identical to, or possibly slightly less radiogenic than the modern mantle. Given their stratigraphic relationship with the surrounding mafic lava flows, the lack of unradiogenic effects in BIFs strengthens the case for an inherited origin of the ^{142}Nd anomalies in volcanic rocks of the Innuisuc complex.

5.2. Age of the Hadean enriched reservoir

Due to the short lifetime of ^{146}Sm , the presence of ^{142}Nd heterogeneities in Ukalik/Nuvvuagittuq lavas constitutes straightforward evidence that Hadean material was involved in the genesis of the oldest components of the Inukjuak domain. More quantitative age constraints cannot be derived from the slope of the ^{146}Sm – ^{142}Nd array, as the latter reflects a mixture of Hadean and Eoarchean components and is therefore chronologically meaningless. Nevertheless, a model age of differentiation can be derived for the Hadean enriched precursor, using a combination of the ^{146}Sm – ^{142}Nd and ^{147}Sm – ^{143}Nd chronometers (e.g. Caro, 2011). Model age calculations using the coupled $^{146,147}\text{Sm}$ – $^{142,143}\text{Nd}$ system have the advantage of being solely based on the isotopic composition of the rocks and do not rely on their Sm/Nd ratios. Using a simple set of chronometric equations, $^{146,147}\text{Sm}$ – $^{142,143}\text{Nd}$ systematics can provide a model age of differentiation (T_d) and an estimate of the time-integrated $^{147}\text{Sm}/^{144}\text{Nd}$ ratio of the reservoir in which the ^{142}Nd anomaly was initially produced.

Following previous $^{146,147}\text{Sm}$ – $^{142,143}\text{Nd}$ studies, we make the simplifying assumption that the Hadean reservoir carrying the ^{142}Nd anomaly was generated at time T_d from an initially primitive mantle, and subsequently evolved as closed system until it was sampled in the Eoarchean, when ^{146}Sm was no longer extant. We consider an eruption age of 3.75 Ga for Ukalik lavas, as inferred from previous U–Pb zircon studies in the NSB (Augland and David, 2015; Cates and Mojzsis, 2007; Cates et al., 2013; David et al., 2006), and use the composition of IN12032 ($\mu^{142}\text{Nd} = -9.8$ ppm and $\varepsilon^{143}\text{Nd}_i = -2$) as the closest approximation of the Hadean component. With these input parameters, the model age of differentiation for the Ukalik enriched source is estimated to be $4.36^{+0.05}_{-0.06}$ Ga (or $4.44^{+0.03}_{-0.04}$ Ga using a 68 Ma half-life for ^{146}Sm). By comparison, the Isua mantle source is estimated to have differentiated $4.42^{+0.05}_{-0.06}$ Ga ago (Caro et al., 2006; Rizo et al., 2011), which is only marginally older than the estimated age of crystallization of the lunar magma ocean, at $4.39^{+0.016}_{-0.014}$ Ga (McLeod et al., 2014). As shown in Fig. 7, a regression including the $^{142,143}\text{Nd}$ data for Ukalik and Isua supracrustal belts yields an age of $4.39^{+0.04}_{-0.035}$ Ga, which is similar to the model age derived from IN12032 and virtually identical to the estimated age of differentiation of the lunar mantle.

It is important to recognize that the chronological information derived from $^{146,147}\text{Sm}$ – $^{142,143}\text{Nd}$ systematics is a model age and, as such, depends on the compositional model assumed for the Bulk Silicate Earth (BSE). The ages provided above were calculated assuming that the BSE has a chondritic Sm/Nd ratio ($^{147}\text{Sm}/^{144}\text{Nd} = 0.1960$, Bouvier et al., 2008) and a $^{142}\text{Nd}/^{144}\text{Nd}$ ratio identical to that of the modern mantle (i.e. $\mu^{142}\text{Nd}_{\text{BSE}} = 0$). However, alterna-

tive models involving slightly superchondritic Sm/Nd compositions have been proposed based on the meteoritic ^{142}Nd record (e.g. Boyet and Gannoun, 2013; Caro et al., 2008; Jackson and Jellinek, 2013; O'Neill and Palme, 2008; Qin et al., 2011; Caro, 2015). As shown in Fig. 7B, a superchondritic Sm/Nd ratio for the BSE would tend to generate older model ages for the Isua depleted source, and younger ages for the Ukalik enriched source. Therefore, the apparent synchronous differentiation of Ukalik and Isua parent reservoirs remains, to a certain extent, model dependent. Solving this issue requires precise assessment of the role of nucleosynthetic vs. radiogenic processes in generating the chondritic ^{142}Nd signal, which is analytically challenging due to the small magnitude of the measured anomalies. Recent studies suggest that the offset between the terrestrial and chondritic $^{142}\text{Nd}/^{144}\text{Nd}$ ratios may be entirely accounted for by nucleosynthetic processes (Fukai and Yokoyama, 2016; Burkhardt et al., 2016), in which case the chronological results shown in Fig. 7 would apply. A single, large-scale differentiation event ca. 4.4 Gyr ago would then best account for the $^{142,143}\text{Nd}$ signatures recorded in both the Ukalik/Nuvvuagittuq and Isua rocks.

The presence of positive ^{142}Nd anomalies in the Eoarchean mantle is generally viewed as reflecting magma ocean crystallization in the aftermath of the Moon-forming giant impact (e.g. Caro, 2011; Caro et al., 2005; Debaille et al., 2013; Bennett et al., 2007; Boyet et al., 2003). This interpretation relies on the estimated age of differentiation, which fits independently derived constraints on the timescale of terrestrial accretion, as well as the apparent decoupling of the Lu-Hf and Sm-Nd systems in the Isua mantle source; an expected outcome of Mg-perovskite crystallization in a deep magma ocean (Caro et al., 2005; Rizo et al., 2011). A synchronous differentiation of the Ukalik and Isua sources would thus imply contamination of Ukalik lavas by material derived from Earth's primordial crust, more than 600 Myr after solidification of the magma ocean. The emplacement of such long-lived, compositionally buoyant lithosphere has been theorized based on parameterized and numerical convection models (Korenaga, 2006; O'Neill et al., 2013; van Hunen and van den Berg, 2008). Due to the sparsity of Hadean components in the geological record, however, its prior existence has proved difficult to substantiate. The chronological constraints derived from $^{146,147}\text{Sm}$ – $^{142,143}\text{Nd}$ systematics suggest that Hadean plates stabilized early, and could be preserved from recycling for a period of time much longer than modern oceanic plates. From a geodynamic viewpoint, this would be consistent with a regime of either stagnant-lid (O'Neill and Debaille, 2014) or sluggish plate tectonics (Foley et al., 2014; Korenaga, 2006), but is seemingly at odds with the occurrence of global resurfacing events, or any mechanism involving rapid rejuvenation of the Hadean surface. Overall, our results suggest that hotter mantle temperatures in the Hadean induced a relatively quiescent tectonic regime, characterized by inefficient lithospheric recycling and a long crustal residence time. This quiescent regime, in turn, allowed remnants of Earth's primordial crust to contribute to the genesis of continental terranes in the Eoarchean.

5.3. Composition of the Hadean enriched reservoir

We now turn from the chronological to the petrogenetic implications of our results, focusing on the nature of the Hadean protolith. Of potential importance to this issue is the observation that $\mu^{142}\text{Nd}$ in Ukalik lavas show a high degree of covariation with Th/La (Fig. 8A), a trace element ratio usually exhibiting limited variability in mafic lithologies, with the notable exception of arc magmas (Plank, 2005). As Th and La are both highly incompatible, they exhibit similar behavior during partial melting and only experience fractionation during crustal differentiation processes. As a result, the upper crust is characterized by high Th/La (0.25–0.4),

whereas MORBs and most OIBs have Th/La < 0.1 (Condie, 1993; Plank, 2005; Taylor and McLennan, 1985). Examination of the Th/La–Sm/La relationships of Fig. 8B shows that tholeiitic lavas have low Th/La irrespective of their Sm/La, as observed in modern MORBs. In contrast, lavas exhibiting ^{142}Nd anomalies show a trend of increasing Th/La with decreasing Sm/La, likely reflecting a mixing relationship between the prevalent Eoarchean mantle (or its melting products) and an enriched end-member similar to the average Archean crust. Thus, Ukalik lavas must have inherited their ^{142}Nd signature from a felsic contaminant, which would be consistent with the reworking of Hadean crustal material in the Innuskuac complex.

By 3.75 Gyr ago, a 4.36 Ga old felsic crust with $^{147}\text{Sm}/^{144}\text{Nd} = 0.08$ – 0.12 would have developed a negative $\mu^{142}\text{Nd}$ of -20 to -30 ppm (Fig. 7A, model A). As shown in Figs. 8A–9, assimilation of such unradiogenic material could readily explain the compositional range of Ukalik amphibolites. Based on these relationships, the trace element composition of IN12032 can be consistently reproduced by ca. 20 wt% assimilation of a TTG contaminant with $\mu^{142}\text{Nd} = -20$ to -30 ppm (Fig. 9B–C). Hence, much of the compositional variability observed in Ukalik lavas could be accounted for by crustal contamination. It is also well established that such mechanism can generate apparent ^{147}Sm – ^{143}Nd dates (and, therefore, ^{146}Sm – ^{142}Nd dates) well in excess of true emplacement ages, as illustrated by several case studies of Archean mafic and ultramafic suites (Chauvel et al., 1985; Juteau et al., 1988).

The crustal assimilation model, however, faces several difficulties. First, despite the seemingly simple relationships of Fig. 9, neither the boninitic nor the transitional lavas can be generated by crustal contamination starting from the most primitive tholeiitic composition. This is most evident for boninitic lavas, which exhibit Mg contents higher than tholeiitic lavas, as well as lower abundances of incompatible elements despite higher SiO_2 contents. Second, the crustal assimilation model requires a contaminant with highly negative $\mu^{142}\text{Nd}$. Felsic plutonic rocks currently exposed in the vicinity of the Ukalik belt average -5.6 ± 3.2 ppm and do not represent plausible contaminants, as is evident in a plot of Th/Yb vs. $\mu^{142}\text{Nd}$ (Fig. 9B). Lastly, the negative ^{142}Nd effects observed in the surrounding Voizel TTGs would imply that their parent magmas assimilated pre-existing Hadean felsic crust in proportions ranging from 15 to 25 wt%. The reworking of older continental crust into younger generations of granitoids is not uncommon, but in the present case appears difficult to reconcile with the striking absence of inherited Hadean zircons in these heavily contaminated rocks (David et al., 2006; Cates and Mojzsis, 2007; O'Neill et al., 2013).

An alternative scenario, more consistent with the above observations, is that Ukalik lavas inherited their signature from an Eoarchean felsic component derived from a pre-existing Hadean mafic crust. In this case, the $^{142,143}\text{Nd}$ signature of Ukalik lavas would reflect that of the Hadean precursor, but their high Th/La values would represent a compositional characteristic of the felsic derivatives carrying the negative ^{142}Nd effects. A mafic precursor would be generally consistent with the compositional constraints derived from coupled Sm–Nd systematics (Fig. 7A); using the $^{142,143}\text{Nd}$ signature of the most contaminated sample, the maximum $(^{147}\text{Sm}/^{144}\text{Nd})_{\text{srce}}$ ratio of the Hadean source is estimated to be 0.17, which falls within the compositional range of mafic/ultramafic rocks (0.15–0.20) (Condie, 1993). As shown in Fig. 8D, a 4.36 Ga old mafic crust with $^{147}\text{Sm}/^{144}\text{Nd} = 0.15$ – 0.17 would have developed by 3.75 Ga a $\mu^{142}\text{Nd}$ of -10 to -15 ppm (model B), and its felsic derivatives would plot on the $\mu^{142}\text{Nd}$ –Th/La array defined by Ukalik lavas (model C, Fig. 8C). This scenario would thus satisfy trace element constraints, which require a predominantly felsic contaminant, while circumventing the issues associated with the crustal assimilation model.

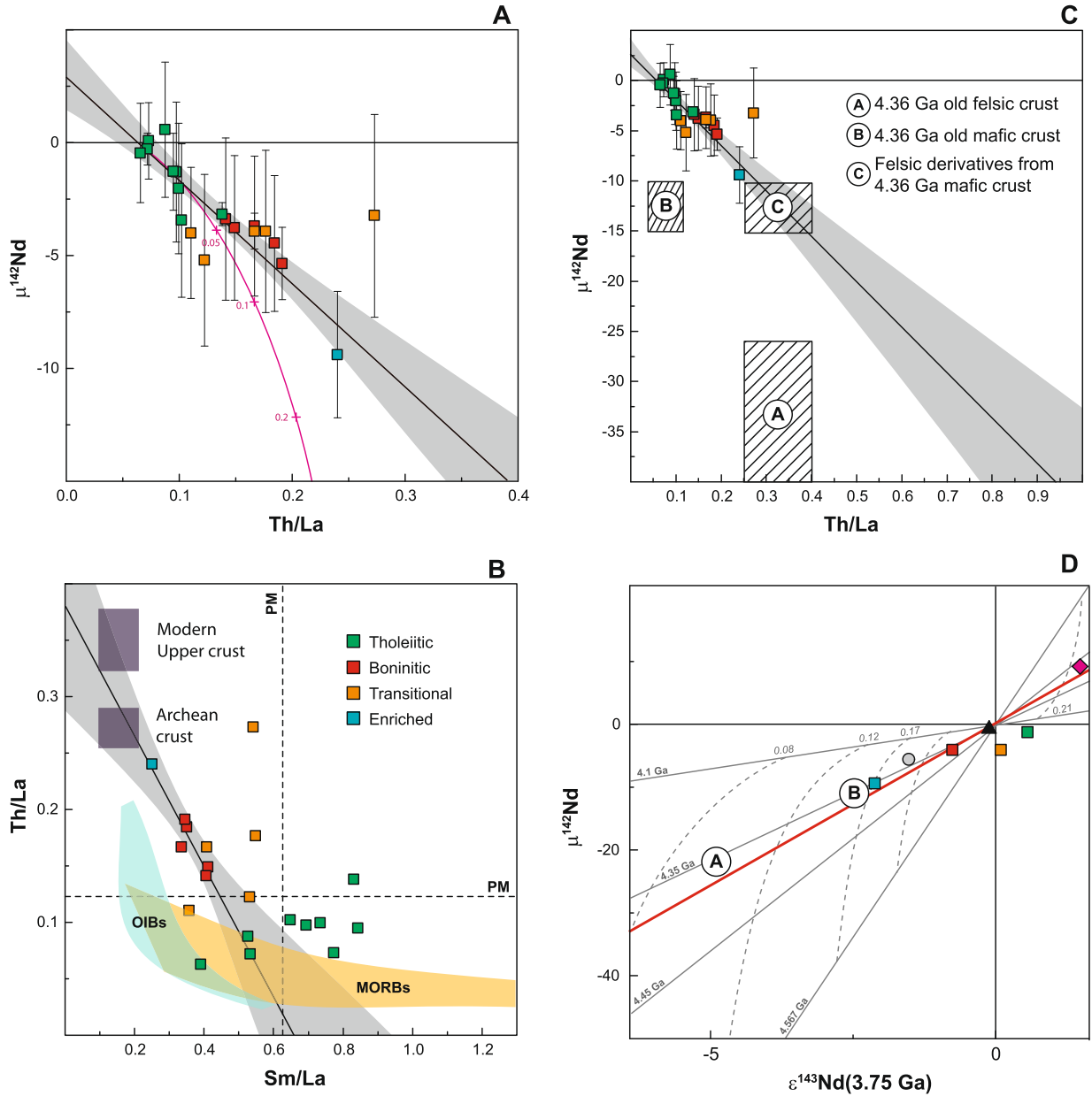


Fig. 8. (A) $\mu^{142}\text{Nd}$ vs. Th/La in amphibolites of the Ukalik belt. The gray field represents the 2 S.D. error envelope for the linear regression obtained from mafic lavas (one datapoint excluded from regression). The pink curve represents a mixing relationship between the most primitive tholeiitic composition and a crustal end-member with $\mu^{142}\text{Nd} = -30$ ppm and a Th/La ratio of 0.26, corresponding to the average Archean crust (Condie, 1993; Taylor and McLennan, 1985). Numbers in pink represent the mass fraction of assimilated felsic crust. (B) Th/La versus Sm/La in Ukalik mafic lavas. The compositional fields for modern MORBs and OIBs (Plank, 2005), as well as the Archean and modern upper continental crust (Condie, 1993; Taylor and McLennan, 1985) are shown for comparison. A linear regression through boninitic and enriched lavas intersects the average composition of the Archean crust, suggesting that the carrier of the negative ^{142}Nd anomalies was a LREE-enriched felsic component. (C) Location of the possible enriched end-members in a $\mu^{142}\text{Nd}$ – $\epsilon^{143}\text{Nd}$ plot. Model A shows the expected composition of 4.36 Ga old felsic crust with $^{147}\text{Sm}/^{144}\text{Nd} = 0.08$ – 0.12 (Condie, 1993; Taylor and McLennan, 1985). Model B represents the composition of a 4.36 Ga mafic crust with $^{147}\text{Sm}/^{144}\text{Nd} = 0.15$ – 0.17 . (D) Location of proposed Hadean end-members in a $\mu^{142}\text{Nd}$ vs. Th/La diagram. Model C shows the expected composition of felsic products derived from a 4.36 Ga mafic crust, after extinction of ^{146}Sm . (For interpretation of the references to color in this figure legend, the reader is referred to the web version of this article.)

The scenarios mentioned above are expected to generate identical effects with regards to trace elements. However, they differ in that a Hadean mafic precursor (and its felsic derivatives (model C)) would have less negative $\mu^{142}\text{Nd}$ than a felsic crust of the same age (model A). Consequently, a crustal contamination scenario using model C as enriched end-member would require larger amount (>40 wt%) of assimilation to account for the signature of IN12032. The $\mu^{142}\text{Nd}$ –Th/La systematics of Ukalik rocks, alternatively, could result from metasomatic enrichment of a depleted or primitive mantle reservoir, prior to extraction of their parent magmas. The isotopic signature of Ukalik lavas would then

require adding 2–10 wt% of a tonalitic contaminant with $\mu^{142}\text{Nd} = -15$ ppm to a mantle with initially primitive abundances of REE.

A key observation in support of a metasomatically enriched mantle source is the widespread occurrence of lavas with boninitic affinities in the Nuvvuagittuq/Ukalik belts. Boninites are subduction-related volcanic rocks characterized by high SiO_2 (>52 wt%), high MgO (>8 wt%) and low TiO_2 (<0.5 wt%) contents (Crawford et al., 1989; Hickey and Frey, 1982). Their characteristic U-shaped REE patterns and overall low abundances of incompatible elements are taken to reflect addition of subduction fluids/melts to a highly refractory mantle, the formation of which is generally attributed

to prior extraction of tholeiitic melts during asthenospheric up-lift associated with trench retreat or back-arc spreading (König et al., 2010; Bedard, 1999; Hickey and Frey, 1982). The presence

of lavas sharing the geochemical characteristics of modern boninite/tholeiite associations in the NSB has been emphasized in several previous studies (O'Neil et al., 2011; Turner et al., 2014), but the implication of this result for Sm–Nd systematics has received surprisingly little attention. Of central importance is the long recognized observation that most boninite suites define positive correlations in a $^{143}\text{Nd}/^{144}\text{Nd}$ vs. Sm/Nd plot (Cameron et al., 1983; Hickey and Frey, 1982; König et al., 2010). These covariations arise from the fact that slab-derived components often contribute >50% of the LREE budget of modern boninites (Cameron et al., 1983; König et al., 2010). A consequence, illustrated in Fig. 10C, is that while tholeiitic magmas in fore arcs or subduction-related ophiolites have $\varepsilon^{143}\text{Nd}$ similar to their coeval mantle, boninites, when present, have variable but always less radiogenic $\varepsilon^{143}\text{Nd}$ largely inherited from the subducting plate.

It is unclear whether the geochemical features illustrated in Fig. 10 must imply the existence of modern-type subduction processes in the Eoarchean, or could have been generated in drip-like downwellings. Nevertheless, in the absence of plausible contaminants in the Innuksuac complex, the isotopic and geochemical characteristics of Ukaliq lavas point towards metasomatic enrichment of a variably depleted Eoarchean mantle as the most plausible scenario for explaining the Innuksuac ^{146}Sm – ^{142}Nd array. This inherited signature, in turn, establishes a clear genetic relationship between the foundering of Earth's primordial crust and the emplacement of both plutonic and volcanic rocks in the Innuksuac complex.

6. Conclusions

An intense debate has surrounded the ^{146}Sm – ^{142}Nd signature characterizing volcanic rocks of the Nuvvuagittuq supracrustal belt, following O'Neil et al.'s proposal to assign a Hadean emplacement age to the sequence. The highly altered nature of the mafic lithologies carrying the ^{142}Nd anomalies, however, has been an obstacle to geochronological investigations in the NSB, and has led to diverging interpretations of their isotopic record. In this study, we investigated the $^{146,147}\text{Sm}$ – $^{142,143}\text{Nd}$ systematics of volcanic and sedimentary rocks from the Ukaliq supracrustal belt, a newly discovered volcano-sedimentary enclave of the Innuksuac complex. Mafic lavas of the USB lack evidence of the hydrothermal alteration that massively modified the chemistry of Nuvvuagittuq rocks and, overall, are in a better state of preservation. They nevertheless display a similar geochemical “flavor”, characterized by the association of arc-type volcanic rocks with variably negative ^{142}Nd anomalies. Despite a rough correlation between the $^{142}\text{Nd}/^{144}\text{Nd}$ and Sm/Nd ratios, the fine structure of the ^{146}Sm – ^{142}Nd signal in Ukaliq rocks is inconsistent with a Hadean emplacement age. ^{142}Nd anomalies are primarily carried by boninitic lavas, likely signaling metasomatic enrichment at mantle depth, whereas the associated tholeiitic and ultramafic rocks have normal $^{142}\text{Nd}/^{144}\text{Nd}$ regardless of their Sm/Nd ratio. More importantly, chemical sediments interleaved in the Nuvvuagittuq and Ukaliq sequences lack the negative anomalies that, given their low Sm/Nd ratio, would be expected had these sediments been deposited in the Hadean.

Coupled $^{146,147}\text{Sm}$ – $^{142,143}\text{Nd}$ chronometry indicates that the Ukaliq/Nuvvuagittuq Hadean source was extracted from the mantle

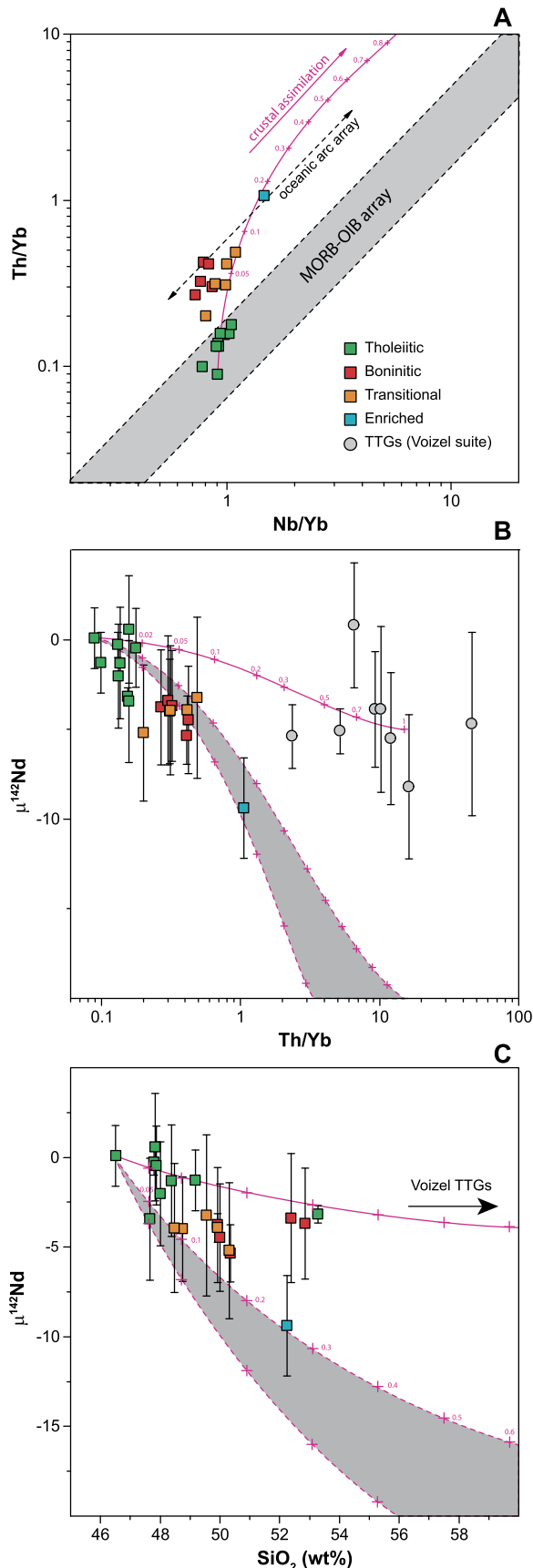


Fig. 9. (A) Th/Yb vs Nb/Th, (B) $\mu^{142}\text{Nd}$ vs Th/Yb and (C) $\mu^{142}\text{Nd}$ vs SiO_2 in mafic lithologies of the Ukaliq belt. The solid pink curves represent mixing relationships between the most primitive tholeiitic composition and a crustal component defined by the average of our analyses of Voizel TTGs. The gray fields in panel (B) and (C) represent the compositional range for tholeiitic magmas contaminated by a 4.36 Ga tonalitic crust with $\mu^{142}\text{Nd}$ ranging from –20 ppm (upper dashed curve) to –30 ppm (lower dashed curve). Numbers in italic represent the mass fraction of assimilated felsic material. (For interpretation of the references to color in this figure legend, the reader is referred to the web version of this article.)

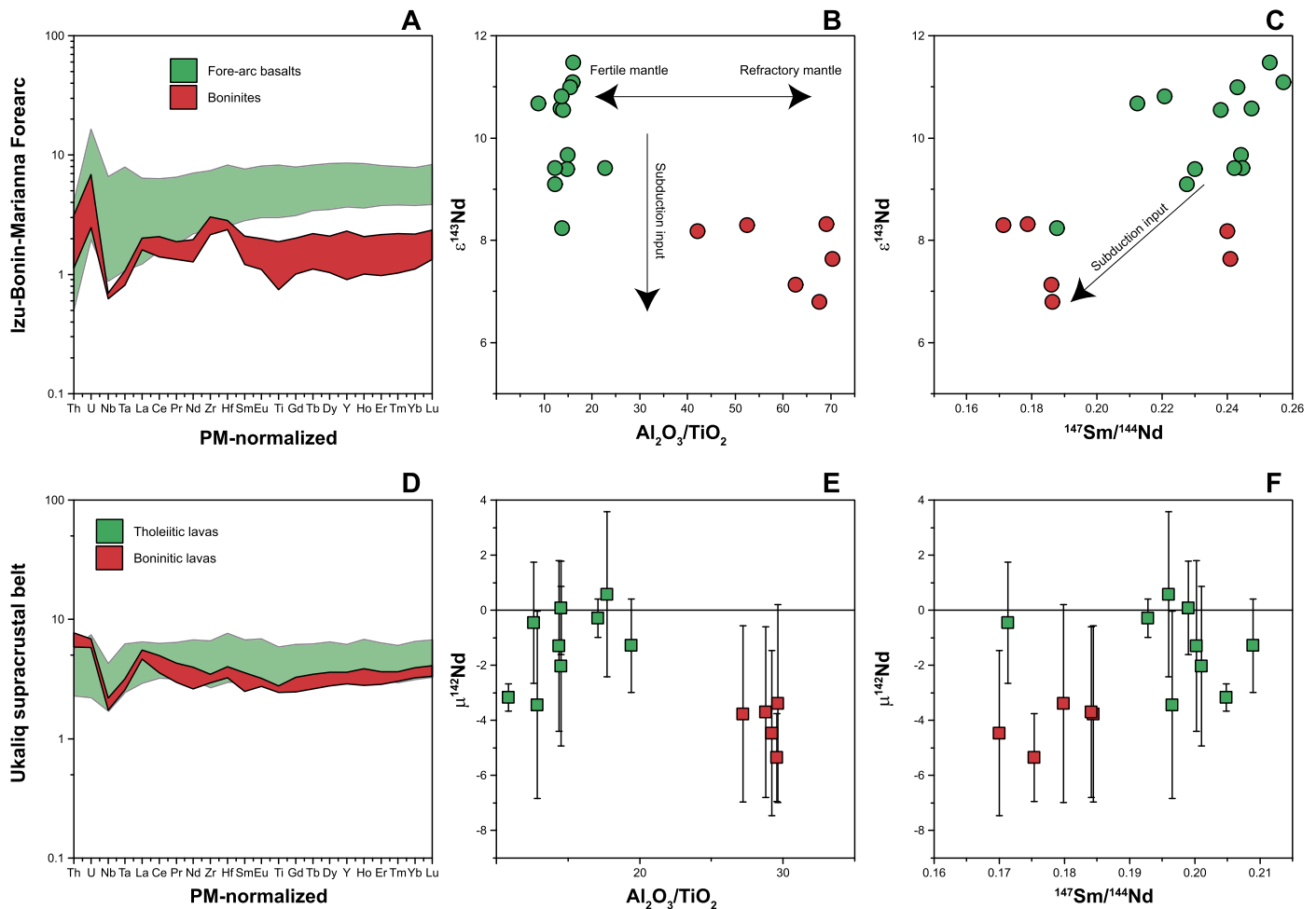


Fig. 10. Trace element and isotopic systematics of boninites and tholeiitic basalts in the Marianna fore-arc (A–C), compared to those of the boninitic and tholeiitic groups in the Ukaliq belt (C–D). Data for the Marianna fore arc lavas are from Reagan et al. (2010). Similar relationships were also reported from several boninite suites worldwide (Cameron et al., 1983; Hickey and Frey, 1982; König et al., 2010). (For interpretation of the colors in this figure, the reader is referred to the web version of this article.)

ca. 4.4 Gyr ago, possibly as a result of magma ocean crystallization, and had a predominantly mafic composition. We propose that foundering of this primordial crust after a long period of quiescence at the surface produced felsic melts and/or fluids carrying unradiogenic $^{142,143}\text{Nd}$ which imprinted the overlying mantle with a chemically and isotopically enriched signature. Metasomatically triggered melting of this modified mantle then generated a variety of boninitic and tholeiitic magmas, the combination of which resulted in the ^{146}Sm – ^{142}Nd pseudo-isochrons observed in Ukaliq and Nuvvuagittuq lavas. Beyond their chronological implications, our results provide clear observational evidence for the emplacement of a long-lived lithosphere following solidification of the terrestrial magma ocean. This observation suggests that hotter internal temperatures did not impede the stabilization of Hadean plates. Rather, they reduced the efficiency of lithospheric recycling and favored a more sluggish tectonic style in the post-magma ocean Earth.

Acknowledgements

We thank Dr. Igor Puchtel and an anonymous reviewer for their constructive comments of this paper. Logistical assistance from the Pituvik Landholding Corporation of Nunavik is gratefully acknowledged. Sarah Davey is thanked for assisting with the 2014 fieldwork. A. Schumacher and C. Zimmermann provided assistance with TIMS and ICP-MS work. GC acknowledges financial support from Agence Nationale de la Recherche (Grant ANR-11-JS56-0012

“DESIR”). P.M. was supported by a doctoral fellowship awarded by Région Lorraine. SJM was supported in this work by the NASA Exobiology Program (14-EXO14_2-0050), and from the Collaborative for Research in Origins (CRiO) at the University of Colorado Boulder, which is funded by the John Templeton Foundation-FfAME Origins program (grant id# 15-09-0168).

Appendix A. Supplementary material

Supplementary material related to this article can be found online at <http://dx.doi.org/10.1016/j.epsl.2016.09.051>.

References

- Arndt, N., Leshner, M., Barnes, S.J., 2008. Komatiite. Cambridge University Press, Cambridge, U.K.
- Augland, L.E., David, J., 2015. Protocrustal evolution of the Nuvvuagittuq Supracrustal Belt as determined by high precision zircon Lu–Hf and U–Pb isotope data. Earth Planet. Sci. Lett. 428, 162–171. <http://dx.doi.org/10.1016/j.epsl.2015.07.039>.
- Bedard, J.H., 1999. Petrogenesis of boninites from the betts cove ophiolite, Newfoundland, Canada: identification of subducted source components. J. Petrol. 40, 1853–1889.
- Bédard, J.H., Brouillette, P., Madore, L., Berclaz, A., 2003. Archaean cratonization and deformation in the northern Superior Province, Canada: an evaluation of plate tectonic versus vertical tectonic models. Precambrian Res. 127, 61–87. [http://dx.doi.org/10.1016/S0301-9268\(03\)00181-5](http://dx.doi.org/10.1016/S0301-9268(03)00181-5).
- Bennett, V.C., Brandon, A.D., Nutman, A.P., 2007. Coupled ^{142}Nd – ^{143}Nd isotopic evidence for Hadean mantle dynamics. Science 318, 1907–1910.

- Bourdon, B., Caro, G., 2007. The early terrestrial crust. *C. R. Géosci.* 339, 928–936. <http://dx.doi.org/10.1016/j.crte.2007.09.002>.
- Bouvier, A., Vervoort, J.D., Patchett, P.J., 2008. The Lu–Hf and Sm–Nd isotopic composition of CHUR: constraints from unequilibrated chondrites and implications for the bulk composition of terrestrial planets. *Earth Planet. Sci. Lett.* 273, 48–57. <http://dx.doi.org/10.1016/j.epsl.2008.06.010>.
- Boyett, M., Carlson, R.W., 2005. ^{142}Nd evidence for early (>4.53 Ga) global differentiation of the silicate Earth. *Science* 309, 576–581. <http://dx.doi.org/10.1126/science.1113634>.
- Boyett, M., Blichert-Toft, J., Rosing, M., Storey, M., Télouk, P., Albarède, F., 2003. ^{142}Nd evidence for early Earth differentiation. *Earth Planet. Sci. Lett.* 214, 427–442. [http://dx.doi.org/10.1016/S0012-821X\(03\)00423-0](http://dx.doi.org/10.1016/S0012-821X(03)00423-0).
- Boyett, M., Gannoun, A., 2013. Nucleosynthetic Nd isotope anomalies in primitive enstatite chondrites. *Geochim. Cosmochim. Acta* 121, 652–666. <http://dx.doi.org/10.1016/j.gca.2013.07.036>.
- Burkhardt, C., Borg, L.E., Brennecka, G.A., Shollenberger, Q.R., Dauphas, N., Kleine, T., 2016. A nucleosynthetic origin for the Earth's anomalous ^{142}Nd composition. *Nature* 537, 394–398. <http://dx.doi.org/10.1038/nature18956>.
- Cameron, W.E., McCulloch, M.T., Walker, D.A., 1983. Boninite petrogenesis: chemical and Nd–Sr isotopic constraints. *Earth Planet. Sci. Lett.* 65, 75–89. [http://dx.doi.org/10.1016/0012-821X\(83\)90191-7](http://dx.doi.org/10.1016/0012-821X(83)90191-7).
- Caro, G., 2015. Chemical geodynamics in a non-chondritic Earth. In: Khan, A., Descamps, F. (Eds.), *The Earth's Heterogeneous Mantle*. Springer Geophysics, pp. 329–366.
- Caro, G., 2011. Early silicate Earth differentiation. *Annu. Rev. Earth Planet. Sci.* 39, 31–58. <http://dx.doi.org/10.1146/annurev-earth-040610-133400>.
- Caro, G., Bourdon, B., Birck, J.L., Moorbath, S., 2006. High-precision $^{142}\text{Nd}/^{144}\text{Nd}$ measurements in terrestrial rocks: constraints on the early differentiation of the Earth's mantle. *Geochim. Cosmochim. Acta* 70, 164–191. <http://dx.doi.org/10.1016/j.gca.2005.08.015>.
- Caro, G., Bourdon, B., Birck, J.-L., Moorbath, S., 2003. ^{146}Sm – ^{142}Nd evidence from Isua metamorphosed sediments for early differentiation of the Earth's mantle. *Nature* 423, 428–432. <http://dx.doi.org/10.1038/nature01897>.
- Caro, G., Bourdon, B., Halliday, A.N., Quitté, G., 2008. Super-chondritic Sm/Nd ratios in Mars, the Earth and the Moon. *Nature* 452, 336–339. <http://dx.doi.org/10.1038/nature06760>.
- Caro, G., Bourdon, B., Wood, B.J., Corgne, A., 2005. Trace-element fractionation in Hadean mantle generated by melt segregation from a magma ocean. *Nature* 436, 246–249. <http://dx.doi.org/10.1038/nature03827>.
- Cates, N.L., Mojzsis, S.J., 2009. Metamorphic zircon, trace elements and Neoproterozoic metamorphism in the ca. 3.75 Ga Nuvvuagittuq supracrustal belt, Québec (Canada). *Chem. Geol.* 261, 99–114. <http://dx.doi.org/10.1016/j.chemgeo.2009.01.023>.
- Cates, N.L., Mojzsis, S.J., 2007. Pre-3750 Ma supracrustal rocks from the Nuvvuagittuq supracrustal belt, northern Québec. *Earth Planet. Sci. Lett.* 255, 9–21. <http://dx.doi.org/10.1016/j.epsl.2006.11.034>.
- Cates, N.L., Ziegler, K., Schmitt, A.K., Mojzsis, S.J., 2013. Reduced, reused and recycled: detrital zircons define a maximum age for the Eoarchean (ca. 3750–3780 Ma) Nuvvuagittuq Supracrustal Belt, Québec (Canada). *Earth Planet. Sci. Lett.* 362, 283–293. <http://dx.doi.org/10.1016/j.epsl.2012.11.054>.
- Chauvel, C., Dupré, B., Jenner, G.A., 1985. The Sm–Nd age of Kambalda volcanics is 500 Ma too old! *Earth Planet. Sci. Lett.* 74, 315–324. [http://dx.doi.org/10.1016/S0012-821X\(85\)80003-0](http://dx.doi.org/10.1016/S0012-821X(85)80003-0).
- Condie, K.C., 1993. Chemical composition and evolution of the upper continental crust: contrasting results from surface samples and shales. *Chem. Geol.* 104, 1–37. [http://dx.doi.org/10.1016/0009-2541\(93\)90140-E](http://dx.doi.org/10.1016/0009-2541(93)90140-E).
- Crawford, A.J., Fallon, T.J., Green, D.H., 1989. Classification, petrogenesis and tectonic setting of boninites. In: Crawford, A.J. (Ed.), *Boninites*, pp. 1–49.
- Darling, J.R., Moser, D.E., Heaman, L.M., Davis, W.J., O'Neil, J., Carlson, R., 2013. Eoarchean to Neoproterozoic evolution of the Nuvvuagittuq Supracrustal belt: new insights from U–Pb zircon geochronology. *Am. J. Sci.* 313, 844–876. <http://dx.doi.org/10.2475/09.2013.02>.
- David, J., Godin, L., Stevenson, R.K., O'Neil, J., Francis, D., 2006. U–Pb ages (3.8–2.7 Ga) and Nd isotope data from the newly identified Eoarchean Nuvvuagittuq supracrustal belt, Superior Craton, Canada. *Geol. Soc. Am. Bull.* 121, 150–163. <http://dx.doi.org/10.1130/B26369.1>.
- Debaille, V., O'Neill, C., Brandon, A.D., Haenecour, P., Yin, Q.-Z., Mattioli, N., Treiman, A.H., 2013. Stagnant-lid tectonics in early Earth revealed by ^{142}Nd variations in late Archean rocks. *Earth Planet. Sci. Lett.* 373, 83–92. <http://dx.doi.org/10.1016/j.epsl.2013.04.016>.
- Foley, B.J., Bercowski, D., Elkins-Tanton, L.T., 2014. Initiation of plate tectonics from post-magma ocean thermochemical convection. *J. Geophys. Res., Solid Earth* 119 (B5), 8561.
- Fukui, R., Yokoyama, T., 2016. Nucleosynthetic Neodymium isotope anomalies in carbonaceous and ordinary chondrites. *Lunar Planet. Sci. Conf. Abstr.* 47, 1298.
- Guitreau, M., Blichert-Toft, J., Mojzsis, S.J., Roth, A.S.G., Bourdon, B., 2013. A legacy of Hadean silicate differentiation inferred from Hf isotopes in Eoarchean rocks of the Nuvvuagittuq supracrustal belt (Québec, Canada). *Earth Planet. Sci. Lett.* 362, 171–181. <http://dx.doi.org/10.1016/j.epsl.2012.11.055>.
- Guitreau, M., Blichert-Toft, J., Mojzsis, S.J., Roth, A.S.G., Bourdon, B., Cates, N.L., Bleeker, W., 2014. Lu–Hf isotope systematics of the Hadean–Eoarchean Acasta Gneiss Complex (Northwest Territories, Canada). *Geochim. Cosmochim. Acta* 135, 251–269. <http://dx.doi.org/10.1016/j.gca.2014.03.039>.
- Harper, C.L., Jacobsen, S.B., 1992. Evidence from coupled ^{147}Sm – ^{143}Nd and ^{146}Sm – ^{142}Nd systematics for very early (4.5-Gyr) differentiation of the Earth's mantle. *Nature* 360, 728–732. <http://dx.doi.org/10.1038/360728a0>.
- Harrison, T.M., 2009. The Hadean crust: evidence from >4 Ga zircons. *Annu. Rev. Earth Planet. Sci.* 37, 479–505. <http://dx.doi.org/10.1146/annurev.earth.031208.100151>.
- Hickey, R.L., Frey, F.A., 1982. Geochemical characteristics of boninite series volcanics: implications for their source. *Geochim. Cosmochim. Acta* 46, 2099–2115. [http://dx.doi.org/10.1016/0016-7037\(82\)90188-0](http://dx.doi.org/10.1016/0016-7037(82)90188-0).
- Jackson, M.G., Jellinek, A.M., 2013. Major and trace element composition of the high $^3\text{He}/^4\text{He}$ mantle: implications for the composition of a nonchondritic Earth. *Geochim. Geophys. Geosyst.* 14, 2954–2976. <http://dx.doi.org/10.1002/ggge.20188>.
- Johnson, T.E., Brown, M., Kaus, B.J.P., VanTongeren, J.A., 2013. Delamination and recycling of Archaean crust caused by gravitational instabilities. *Nat. Geosci.* 7, 47–52. <http://dx.doi.org/10.1038/ngeo2019>.
- Juteau, M., Pagel, M., Michard, A., Albarede, F., 1988. Assimilation of continental crust by komatiites in the Precambrian basement of the Carswell structure (Saskatchewan, Canada). *Contrib. Mineral. Petrol.* 99, 219–225. <http://dx.doi.org/10.1007/BF00371462>.
- Kinoshita, N., Paul, M., Kashiv, Y., Collon, P., Deibel, C.M., DiGiovine, B., Greene, J.P., Henderson, D.J., Jiang, C.L., Marley, S.T., Nakanishi, T., Pardo, R.C., Rehm, K.E., Robertson, D., Scott, R., Schmitt, C., Tang, X.D., Vondrasek, R., Yokoyama, A., 2012. A shorter ^{146}Sm half-life measured and implications for ^{146}Sm – ^{142}Nd chronology in the solar system. *Science* 335, 1614–1617. <http://dx.doi.org/10.1126/science.1215510>.
- König, S., Münker, C., Schuth, S., Luguet, A., Hoffmann, J.E., Kuduon, J., 2010. Boninites as windows into trace element mobility in subduction zones. *Geochim. Cosmochim. Acta* 74, 684–704. <http://dx.doi.org/10.1016/j.gca.2009.10.011>.
- Korenaga, J., 2006. Archean geodynamics and the thermal evolution of Earth. In: *Archean Geodynamics and Environments*, vol. 164, pp. 7–32.
- Le Bas, M.J., 2000. IUGS reclassification of the high-mg and picritic volcanic rocks. *J. Petrol.* 41, 1467–1470. <http://dx.doi.org/10.1093/petrology/41.10.1467>.
- Ludwig, K.R., 1991. ISOPLLOT: a plotting and regression program for radiogenic-isotope data; version 2.53. Open-File Rep.
- Marks, N.E., Borg, L.E., Hutcheon, I.D., Jacobsen, B., Clayton, R.N., 2014. Samarium–neodymium chronology and rubidium–strontium systematics of an Allende calcium–aluminum-rich inclusion with implications for ^{146}Sm half-life. *Earth Planet. Sci. Lett.* 405, 15–24. <http://dx.doi.org/10.1016/j.epsl.2014.08.017>.
- McLeod, C.L., Brandon, A.D., Armitage, R.M.G., 2014. Constraints on the formation age and evolution of the Moon from ^{142}Nd – ^{143}Nd systematics of Apollo 12 basalts. *Earth Planet. Sci. Lett.* 396, 179–189. <http://dx.doi.org/10.1016/j.epsl.2014.04.007>.
- Meissner, F., Schmidt-Ott, W.-D., Ziegler, L., 1987. Half-life and α -ray energy of ^{146}Sm . *Z. Phys., A At. Nucl.* 327, 171–174. <http://dx.doi.org/10.1007/BF01292406>.
- Moskowska, A.M., Mojzsis, S.J., Pecoits, E., Papineau, D., Dauphas, N., Konhauser, K.O., 2013. Chemical sedimentary protoliths in the >3.75 Ga Nuvvuagittuq Supracrustal Belt (Québec, Canada). *Gondwana Res.* 23, 574–594. <http://dx.doi.org/10.1016/j.gr.2012.11.005>.
- Moskowska, A.M., Pecoits, E., Cates, N.L., Mojzsis, S.J., O'Neil, J., Robbins, L.J., Konhauser, K.O., 2012. The composition of Earth's oldest iron formations: The Nuvvuagittuq Supracrustal Belt (Québec, Canada). *Earth Planet. Sci. Lett.* 317–318, 331–342. <http://dx.doi.org/10.1016/j.epsl.2011.11.020>.
- Mojzsis, S.J., Cates, N.L., Caro, G., Trail, D., Abramov, O., Guitreau, M., Blichert-Toft, J., Hopkins, M., Bleeker, W., 2014. Component geochronology in the polyphase ca. 3920 Ma Acasta Gneiss. *Geochim. Cosmochim. Acta* 133, 68–96. <http://dx.doi.org/10.1016/j.gca.2014.02.019>.
- Mojzsis, S.J., Harrison, T.M., Pidgeon, R.T., 2001. Oxygen-isotope evidence from ancient zircons for liquid water at the Earth's surface 4,300 Myr ago. *Nature* 409, 178–181. <http://dx.doi.org/10.1038/35051557>.
- O'Neill, J., Carlson, R.W., Francis, D., Stevenson, R.K., 2008. Neodymium-142 evidence for Hadean mafic crust. *Science* 321, 1828–1831.
- O'Neill, J., Carlson, R.W., Paquette, J.-L., Francis, D., 2012. Formation age and metamorphic history of the Nuvvuagittuq Greenstone Belt. *Precambrian Res.* 220–221, 23–44. <http://dx.doi.org/10.1016/j.precamres.2012.07.009>.
- O'Neill, J., Francis, D., Carlson, R.W., 2011. Implications of the Nuvvuagittuq Greenstone Belt for the Formation of Earth's Early Crust. *J. Petrol.* 52, 985–1009. <http://dx.doi.org/10.1093/petrology/egr014>.
- O'Neill, J., Maurice, C., Stevenson, R.K., Larocque, J., Cloquet, C., David, J., Francis, D., 2007. The Geology of the 3.8 Ga Nuvvuagittuq (Porpoise Cove) Greenstone Belt, Northeastern Superior Province, Canada. In: Van Kranendonk, M.J., Smithies, R.H., Bennett, V.S. (Eds.), *Earth's Oldest Rocks*. Elsevier, pp. 219–250.
- O'Neill, J., Boyett, M., Carlson, R.W., Paquette, J.-L., 2013. Half a billion years of reworking of Hadean mafic crust to produce the Nuvvuagittuq Eoarchean felsic crust. *Earth Planet. Sci. Lett.* 379, 13–25. <http://dx.doi.org/10.1016/j.epsl.2013.07.030>.
- O'Neill, C., Debaille, V., 2014. The evolution of Hadean–Eoarchean geodynamics.

- Earth Planet. Sci. Lett. 406, 49–58. <http://dx.doi.org/10.1016/j.epsl.2014.08.034>.
- O'Neill, C., Debaille, V., Griffin, W., 2013. Deep earth recycling in the Hadean and constraints on surface tectonics. *Am. J. Sci.* 313, 912–932. <http://dx.doi.org/10.2475/09.2013.04>.
- O'Neill, H.S.C., Palme, H., 2008. Collisional erosion and the non-chondritic composition of the terrestrial planets. *Philos. Trans. A, Math. Phys. Eng. Sci.* 366, 4205–4238. <http://dx.doi.org/10.1098/rsta.2008.0111>.
- Plank, T., 2005. Constraints from thorium/lanthanum on sediment recycling at subduction zones and the evolution of the continents. *J. Petrol.* 46, 921–944. <http://dx.doi.org/10.1093/petrology/egi005>.
- Puchtel, I.S., Blichert-Toft, J., Touboul, M., Horan, M.F., Walker, R.J., 2016. The coupled ^{182}W – ^{142}Nd record of early terrestrial mantle differentiation. *Geochem. Geophys. Geosyst.* 17, 2168–2193. <http://dx.doi.org/10.1002/2016GC006324>.
- Qin, L., Carlson, R.W., Alexander, C.M.O., 2011. Correlated nucleosynthetic isotopic variability in Cr, Sr, Ba, Sm, Nd and Hf in Murchison and QUE 97008. *Geochim. Cosmochim. Acta* 75, 7806–7828. <http://dx.doi.org/10.1016/j.gca.2011.10.009>.
- Reagan, M.K., Stern, R.J., Kelley, K.A., Bloomer, S.H., Fryer, P., Hanan, B.B., Vargas, R.H., 2010. Fore – arc basalts and subduction initiation in the Izu–Bonin–Mariana system. *Geochem. Geophys. Geosyst.* 11. <http://dx.doi.org/10.1029/2009GC002871>.
- Rizo, H., Boyet, M., Blichert-Toft, J., O'Neil, J., Rosing, M.T., Paquette, J.-L., 2012. The elusive Hadean enriched reservoir revealed by ^{142}Nd deficits in Isua Archaean rocks. *Nature* 491, 96–100. <http://dx.doi.org/10.1038/nature11565>.
- Rizo, H., Boyet, M., Blichert-Toft, J., Rosing, M., 2011. Combined Nd and Hf isotope evidence for deep-seated source of Isua lavas. *Earth Planet. Sci. Lett.* 312, 267–279. <http://dx.doi.org/10.1016/j.epsl.2011.10.014>.
- Robin, C.M.I., Bailey, R.C., 2009. Simultaneous generation of Archean crust and subcratonic roots by vertical tectonics. *Geology* 37, 523–526. <http://dx.doi.org/10.1130/G25519A.1>.
- Roth, A.S.G., Bourdon, B., Mojzsis, S.J., Rudge, J.F., Guitreau, M., Blichert-Toft, J., 2014. Combined $^{147,146}\text{Sm}$ – $^{143,142}\text{Nd}$ constraints on the longevity and residence time of early terrestrial crust. *Geochem. Geophys. Geosyst.* 15, 2329–2345. <http://dx.doi.org/10.1002/2014GC005313>.
- Roth, A.S.G., Bourdon, B., Mojzsis, S.J., Touboul, M., Sprung, P., Guitreau, M., Blichert-Toft, J., 2013. Inherited ^{142}Nd anomalies in Eoarchean protoliths. *Earth Planet. Sci. Lett.* 361, 50–57. <http://dx.doi.org/10.1016/j.epsl.2012.11.023>.
- Shirey, S.B., Richardson, S.H., 2011. Start of the Wilson Cycle at 3 Ga Shown by Diamonds from Subcontinental Mantle. *Science* 333, 434–436. <http://dx.doi.org/10.1126/science.1206275>.
- Simard, M., Parent, M., David, J., Sharma, K.N.M., 2003. Géologie de la région de la rivière Innusuauc (SNRC 34K et 34L). *Ministères des Ressources Nat. Québec RG* 2002–10.
- Sleep, N.H., Windley, B.F., 1982. Archean plate tectonics: constraints and inferences. *J. Geol.* 90, 363–379. <http://dx.doi.org/10.1086/628691>.
- Stevenson, R., David, J., Parent, M., 2006. Crustal evolution of the western Minto Block, northern Superior Province, Canada. *Precambrian Res.* 145, 229–242. <http://dx.doi.org/10.1016/j.precamres.2005.12.004>.
- Taylor, S.R., McLennan, S.M., 1985. *The Continental Crust: Its Composition and Evolution*. Blackwell Scientific, Oxford.
- Touboul, M., Liu, J., O'Neil, J., Puchtel, I.S., Walker, R.J., 2014. New insights into the Hadean mantle revealed by ^{182}W and highly siderophile element abundances of supracrustal rocks from the Nuvvuagittuq Greenstone Belt, Quebec, Canada. *Chem. Geol.* 383, 63–75. <http://dx.doi.org/10.1016/j.chemgeo.2014.05.030>.
- Turner, S., Rushmer, T., Reagan, M., Moyen, J.-F., 2014. Heading down early on? Start of subduction on Earth. *Geology* 42, 139–142. <http://dx.doi.org/10.1130/G348861>.
- van Hunen, J., van den Berg, A.P., 2008. Plate tectonics on the early Earth: limitations imposed by strength and buoyancy of subducted lithosphere. *Lithos* 103, 217–235. <http://dx.doi.org/10.1016/j.lithos.2007.09.016>.
- Van Thienen, P., van den Berg, A.P., Vlaar, N.J., 2004. Production and recycling of oceanic crust in the early Earth. *Tectonophysics* 386, 41–65. <http://dx.doi.org/10.1016/j.tecto.2004.04.027>.
- Vlaar, N.J., van Keken, P.E., van den Berg, A.P., 1994. Cooling of the earth in the Archaean: consequences of pressure-release melting in a hotter mantle. *Earth Planet. Sci. Lett.* 121, 1–18. [http://dx.doi.org/10.1016/0012-821X\(94\)90028-0](http://dx.doi.org/10.1016/0012-821X(94)90028-0).